Katharina Dirnbauer, BSc

Coffee-based Quinones for Redox Flow Battery Application

MASTER'S THESIS

to achieve the university degree of

Diplom-Ingenieur

Master's degree programme: Technical Chemistry

submitted to

Graz University of Technology

Supervisors

Ass.Prof. Mag.rer.nat. Dr.rer.nat. Stefan Spirk

Dipl.-Ing. Dr.techn. Werner Schlemmer, BSc

Institute of Bioproducts and Paper Technology (BPTI)

Faculty of Technical Chemistry, Chemical and Process Engineering and Biotechnology

Graz, March 2021

Eidesstattliche Erklärung

Ich erkläre an Eides statt, dass ich die vorliegende Arbeit selbstständig verfasst, andere als die angegebenen Quellen/Hilfsmittel nicht benutzt, und die den benutzten Quellen wörtlich und inhaltlich entnommenen Stellen als solche kenntlich gemacht habe. Das in TUGRAZonline hochgeladene Textdokument ist mit der vorliegenden Masterarbeit identisch.

I declare that I have authored this thesis independently, that I have not used any sources/resources other than those indicated, and that I have marked the passages taken from the sources used, both literally and in terms of content, as such. The text document uploaded to TUGRAZonline is identical to the present master thesis.

_____ _____

Datum / Date Unterschrift / Signature

“Nothing in life is to be feared, it is only to be understood. Now is the time to understand more, so that we may fear less.”

MARIE CURIE

Acknowledgements

First of all, I would like to thank Assoc. Prof. Stefan Spirk for supervising my master's thesis and for giving me the opportunity to start work with him in his group. At this point, I would also like to thank Dr. Werner Schlemmer, who co-supervised my work and always gave me good advice and support. Furthermore, special thanks to the whole working group for a lot of advice and shared experiences as well as for the friendly working atmosphere.

A big thanks to Dieter Wurm who brought this exciting project to life. I would like to thank Adelheid Bakhshi and her team for helping me with my work. Special thanks to Silvia Maitz and Herta Luttenberger for doing the GC-MS measurements.

Last but not least, I could not thank my family and friends enough, who have accompanied and supported me during my studies here in Graz. I want to thank my parents for supporting me financially, without putting me under pressure. Special thanks to each and every one of my friends who were there for me when I needed them.

Abstract

One of the most promising batteries in terms of sustainability is the organic redox flow battery (RFB). In addition, several tonnes of coffee waste from the industrial coffee production fill landfills per year due to the popularity of coffee worldwide. The redox-active phenols (chlorogenic acid (CGA), caffeic acid (CA)) contained in this waste can be extracted and used as electrolyte material.

Seven different plant-based sources (spent coffee grounds, coffee silver skins, green beans (*Coffea arabica*), roasted beans (*Coffea arabica*), cocoa shells, abrased coffee and instant coffee) were extracted with a Soxhlet extractor. The extraction was performed with mixtures of ethanol:water (3:2, v:v) and isopropanol:water (3:2, v:v), respectively. A rapid TLC analysis method was developed to determine CGA and CA content. This was compared with GC-MS measurements.

The electrochemical behaviour of *para*-benzoquinone (pBQ), CGA and CA was studied in different molarities of H_3PO_4 and 1 M citric acid and 2 M sodium phosphate dibasic dihydrate buffer system with cyclic voltammetry. The results showed a linear dependency of the peak current i_p and the square root of the scan rate $v^{1/2}$ which indicates a diffusion-controlled mechanism over the investigated pH range. The diffusion coefficients for pBQ, CA and CGA in 0.5 M and in the buffer system were calculated. Also, pBQ, CGA and CA showed quasi-reversibility and two-electron transfer within the used aqueous systems. For the redox flow cell experiments CA and pBQ were used. These materials achieved a capacity of 134 mAh/g at an average of 100% constant coulomb efficiency for 20 cycles.

Kurzfassung

Eine der vielversprechendsten Batterien in Bezug auf die Nachhaltigkeit ist die organische Redox-Flow-Batterie (RFB). Aufgrund der weltweiten Beliebtheit von Kaffee, füllen jährlich mehrere Tonnen Kaffeeabfälle aus der industriellen Kaffeeproduktion die Mülldeponien. Die in diesem Abfall enthaltenen redoxaktiven Phenole (Chlorogensäure (CGA), Kaffeesäure (CA)) können extrahiert und als Elektrolytmaterial verwendet werden.

Sieben pflanzliche Proben (Kaffeesatz, Kaffeesilberhäutchen, grüne Bohnen (Coffea arabica), geröstete Bohnen (Coffea arabica), Kakaoschalen, abgeriebener Kaffee und Instantkaffee) wurden mit einem Soxhlet-Extraktor extrahiert. Die Extraktion wurde mit Mischungen aus Ethanol:Wasser (3:2, v:v) bzw. Isopropanol:Wasser (3:2, v:v) durchgeführt. Zur Bestimmung des CGA- und CA-Gehalts wurde eine schnelle TLC-Analysemethode entwickelt. Diese wurde mit GC-MS-Messungen verglichen.

Das elektrochemische Verhalten von para-Benzochinon (pBQ), CGA und CA wurde in verschiedenen Molaritäten von H_3PO_4 und 1 M Zitronensäure und 2 M Dinatriumhydrogenphosphat-Puffersystem mit zyklischer Voltammetrie untersucht. Die Ergebnisse zeigten eine lineare Abhängigkeit des Spitzenstroms i_p und der Quadratwurzel der Scanrate $v^{1/2}$, was auf einen diffusionskontrollierten Mechanismus über den untersuchten pH-Bereich hinweist. Die Diffusionskoeffizienten für pBQ, CA und CGA in 0,5 M H_3PO_4 und im Puffersystem wurden berechnet. Außerdem zeigten pBQ, CGA und CA Quasi-Reversibilität und Zwei-Elektronen-Transfer in den verwendeten wässrigen Systemen. Für die RFB-Experimente wurden CA und pBQ verwendet. Diese Materialien erreichten eine Kapazität von 134 mAh/g bei einer durchschnittlichen konstanten Coulomb-Effizienz von 100% für 20 Zyklen.

Table of Contents

1 Introduction

1.1 Renewable energy and energy storage

Conventional energy sources (oil, coal, natural gas) are used worldwide. However, these sources are being depleted and the energy demand is steadily increasing. Since more and more environmental companies are becoming active, the research was focused on clean fuel technologies and new energies. In the last years, utilisation of energy from renewable sources has increased. The sun is the greatest source of renewable energies. Its power can be used directly (e.g. thermal, photochemical and photoelectric) and as well as indirectly (e.g. wind, hydropower and photosynthetic energy stored in biomass). In addition, renewable energies are derived from other natural mechanisms on earth (e.g. geothermal and tidal energy) (**Figure 1**). Energy resources derived from fossil fuels, waste products from fossil sources or waste products from inorganic sources are not included. Meanwhile, renewable energy technologies show the ability to provide 3078 times the current energy needs worldwide. Renewable resources are more used in electricity generation than in heat production or transport. Hydro, wind and bioenergy are the main electricity generators.[1]

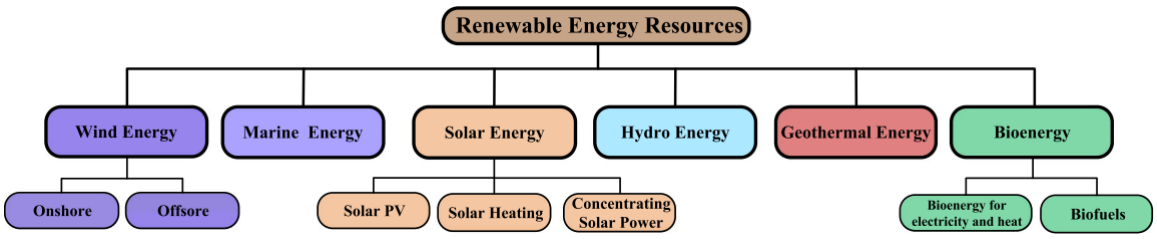

Figure 1: Overview of renewable energy sources.[1]

Fossil energy carriers can be stored easily and used on demand, whereas wind or solar energy depend on weather situations and cannot be stored directly. Therefore, the development and application of energy storage technologies is a crucial factor to store this green energy and replace conventional energy sources. Many types of energy storage systems exist, e.g. they can be categorised in terms of specific energy (Wh/kg) and specific

power (W/kg), known as the 'Ragone plot' (**Figure 2**). The plot helps to identify which system is needed for a certain application. The term energy density describes the energy that can be stored per unit volume or mass and power density is the amount of energy output per unit volume.[2]

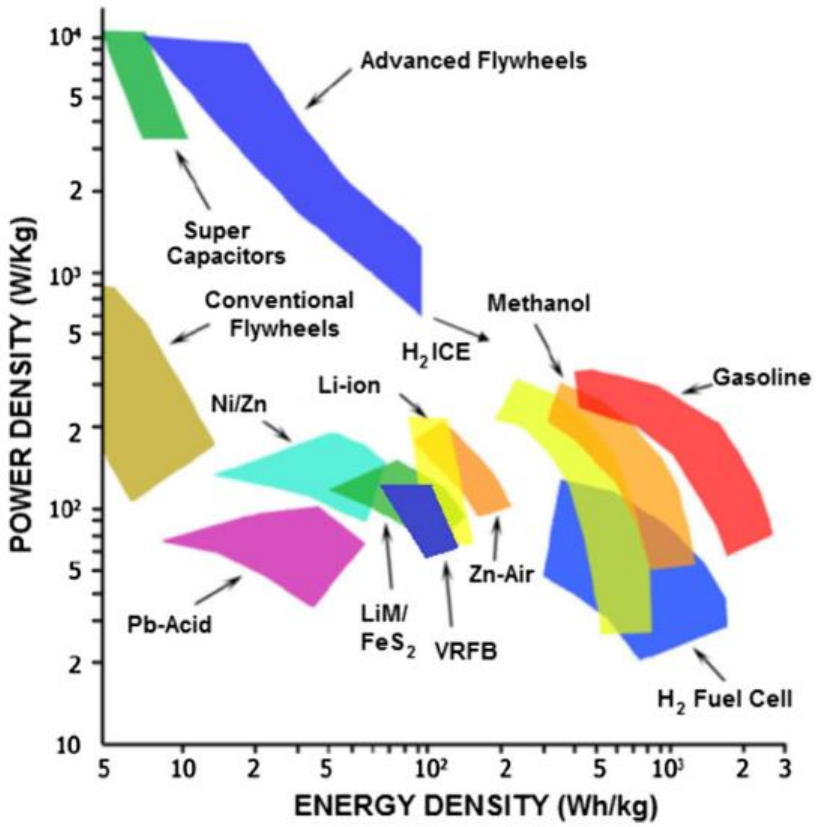

Figure 2: Ragone plot comparing different storage systems.[3]

The commonly used lithium-ion battery has a high energy density and a long life cycle but the cost for lithium is higher than for vanadium. The lead-acid battery is cheap but the life cycles and energy density are much lower than in a lithium battery.[3] The ideal large-scale storage system should have durability for a large number of charge/discharge cycles as well as a long life cycle, high round-trip efficiency, the ability to react quickly to changes and a reasonable price. Among the traditional systems, the secondary redox flow battery (RFB) meets many of these requirements and provides an efficient way to store a large amount of energy.[4]

1.1.1 Redox-flow-batteries (RFB)

Redox-flow batteries (**Figure 3**) consist of two porous electrodes, a separating ion-conductive membrane and two external tanks containing the electrolyte solution. Contrary to traditional batteries where the energy is stored in the active electrode material, in RFBs the energy is stored in two dissolved redox pairs.[5]

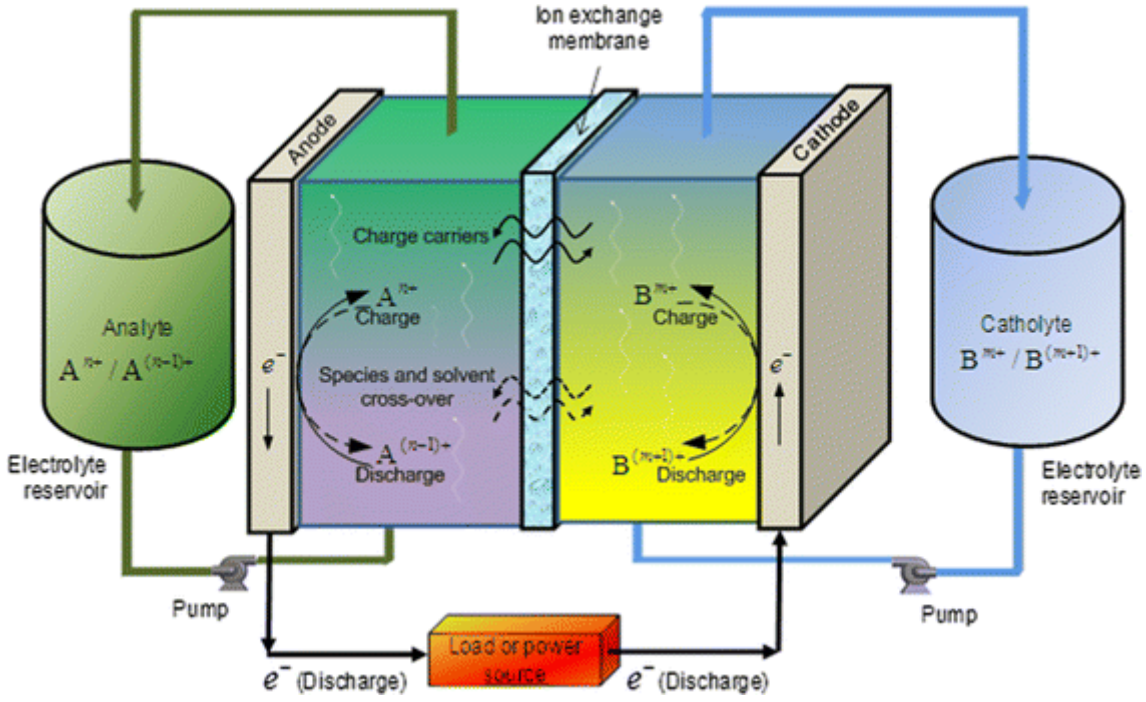

Figure 3: Scheme of a redox flow battery.[4]

RFBs provide reversible conversion between electrical and chemical energy with two soluble redox couples which are dissolved in two external electrolyte tanks. The solutions are pumped to the electrochemical cell, where the charge and discharge process takes place. The redox reactions are reversible which makes this system fully rechargeable. In aqueous systems, the concentration of the electrolyte indicates the specific energy density. Thus, the higher the solubility of the redox couples, the better the system.[5]

The ion exchange membrane (IEM) is one of the most important components of the RFB system. The IEM needs to be stable in the electrolyte. It separates the two electrolyte solutions and only allows the transportation of charged ions. The most common membrane for RFBs is Nafion, a perfluorinated polymer.[5] The advantages of this membrane are the

high proton conductivity, excellent electrochemical properties (high coulombic (93.8%) and voltage efficiency (90.7%) for Nafion 117) and chemical stability (low degradation rate). In addition, the high thermal stability allows a high operating temperature range up to 190 °C. However, there are some drawbacks which includes high cost, fast vanadium ion crossover (permeability of VO^{2+} in Nafion 117: 36.55×10^{-7} cm/min) and a decrease of proton conductance at low humidity or high temperature.[3,6]

The requirements for the electrodes are a high surface area, adequate porosity, low electronic resistance and high electrochemical activity. The most common electrode materials are graphite- or carbon based.[5]

In the mid-1980s the first vanadium RFB (VRFB) was invented by Skyllas-Kazacos research group. This was the generation 1 (G1) VRFB with the following chemical reactions (**Equation 1-4**). This RFB uses the different oxidation states of vanadium. The redox couples V(II)/V(III) and V(IV)/V(V) are used as the anode and cathode, respectively.[3,5]

Cathode:	$VO_2^+ + 2H^+ + e^- \rightleftharpoons VO^{2+} + H_2O$	$E^0 = +1.0$ V	**Equation 1**
Anode:	$V^{2+} \rightleftharpoons V^{3+} + e^-$	$E^0 = -0.26$ V	**Equation 2**
Cell reaction:	$VO_2^+ + V^{2+} + 2H^+ \rightleftharpoons VO^{2+} + V^{3+} + H_2O$	$E^0 = +1.26$ V	**Equation 3**

This all-vanadium redox flow battery is the most common system with a relatively low energy density of 15-25 Wh/kg. Further research led to the generation 2 (G2) battery using a mixture of vanadium chloride and vanadium bromide as electrolyte. The specific energy increased to 25-50 Wh/kg compared to G1. For the third generation (G3) a mixture of H_2SO_4/HCl electrolyte solution was used. This improved the stability and the solubility.[3]

Other metal RFB systems are iron/chromium, polysulfide/bromide, zinc/bromide and vanadium/cerium flow batteries. Also mixed acid vanadium redox flow batteries exist e.g. iron/vanadium.[2,5] Another field of interest are the so called “hybrid” RFBs in which one of the redox couples is in a non-liquid form e.g. a zinc/polyhalide battery.[5]

Advantages of RFBs in general are the possibility to store large amounts of energy up to megawatt hours (MWh). The design is flexible and allows different sizes. While the energy depends on the storage capacity of the electrolyte tanks, the redox couple and its concentration, the power is determined by the reactor size (electrode and membrane surface). Additionally, RFBs offer a long cycle life, the materials are stored separately and, in the case of aqueous RFBs, the main liquid is water. Also, the cells can be arranged in series to increase the cell voltage and a simple scale-up is possible.[4,5]

The disadvantages are the high material costs. Vanadium-based reactants (V_2O_5: \$8.10/lb)[7] and Nafion membranes (\$500 to \$1000 per m^2) increase the cost of all-vanadium RFBs.[5] The performance is limited by the cell operation voltage and active material concentration. The relatively low energy density and toxic electrolyte materials are also a big drawback.[5] In addition, capacity loss can be caused by chemical degradation of redox species.[8]

Challenges of RFBs are the application of new redox couples as anolyte and catholyte with suitable electrolytes and the development of advanced materials. A crucial step will be improving the performance while minimizing cost.[5] Current research topics are finding ways to increase the energy and power density with monolithic electrodes, owning high surface areas and improving the cell design.[2]

1.1.2 Organic redox-flow batteries

The materials for metal acid RFBs are toxic, expensive and limited, so organic compounds have been investigated as a green alternative. Organic sources are abundant on earth and inexpensive. The possibility of molecular modification is a powerful advantage to improve energy and power density. Thus, organic RFBs are a promising clean energy storage system.[9] Ideally, these organic compounds could achieve a specific energy of 150 W/kg or energy density of 210 Wh/L. These are higher values compared to a conventional lithium-ion battery (120 W/kg, 270 Wh/L).[10]

Organic RFB types comprise all-organic redox flow battery (organic redox couple in both sides), organic inorganic redox flow battery (inorganic compound in one side) and organic

inorganic hybrid flow battery (metal deposition or anode in one side). The most common organic RFBs use aqueous- or non-aqueous systems.[10]

A key element of an ideal rechargeable RFBs is the rapid kinetics of the charge-transfer process. Quinones are capable of undergoing proton-coupled electron transfer without dissociation of high energy bonds leading to relatively high rate constants (10^{-3} to 10^{-4} cm/s) and.[11]

An example for the first all-quinone RFB is the one using 1,2-benzoquinone-3,5-disulfonic acid (BQDS) as anolyte (**Equation 4**) and anthraquinone-2,6-disulfonic acid (AQDS) as catholyte (**Equation 5**) with a cell potential of 0.76 V, an energy density of 4.1Wh/L and a low constant cycling for 12 cycles.[10,11]

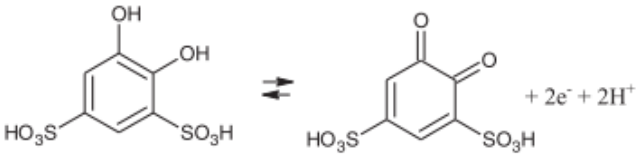

E^0 = +0.85 V **Equation 4**

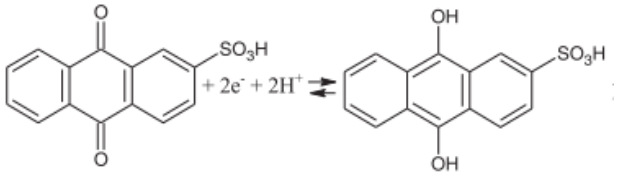

E^0 = +0.09 V **Equation 5**

The organic radical TEMPO (2,2,6,6-tetramethylpiperidinyloxyl) is highly stable due to its delocalised electrons and the steric protection from four methyl groups. Moreover, it shows a fast 1-electron redox reaction and during oxidation it forms an oxoammonium cation ($TEMPO^+$).[9] An aqueous all-organic radical RFB was performed with 4-hydroxy-TEMPO as catholyte (**Equation 7**) and methyl viologen as anolyte (**Equation 6**).[8,10] The addition of an hydroxyl group to TEMPO can shift the redox potential and also increase the solubility in water.[9] This system achieved 1.25 V with an energy density of 8.4 Wh/L and stable cycling for 100 cycles, but lost capacity at higher concentrations.[8,10]

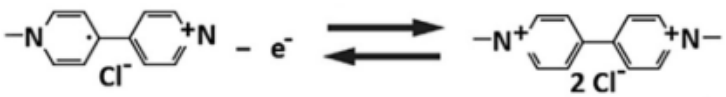

E^0 = -0.45 V **Equation 6**

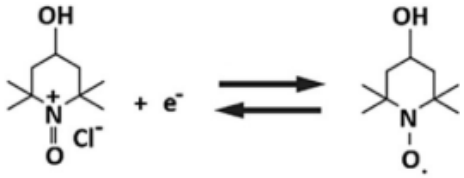

E^0 = +0.80 V **Equation 7**

A recent article reported the utilisation of vanillin (synthesised from lignin) as a source of bio-based quinones. Lignin is naturally occurring in wood and is a by-product from the pulp and paper industry. This makes vanillin a highly available and renewable compound. For this all-quinone redox flow battery, 2-methoxy-1,4-quinone (MQ) was used as anolyte and *para*-benzoquinone (pBQ) as catholyte. The electrolyte solution to stabilise the redox couple was 0.5 M H_3PO_4. This system achieved a high energy density of 27.1 Wh/L and stable cycling for 250 cycles.[12]

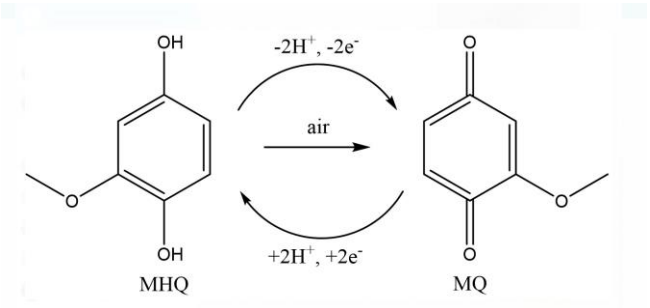

Figure 4: Reduction and oxidation mechanism of 2-methoxy-1,4-hydroquinone (MHQ) and 2-methoxy-1,4-quinone (MQ). respectively.[12]

1.1.3 Quinones

Quinones are organic compounds that are cyclically conjugated diketones. They are carbonyl-based (C=O) and redox active.[9,10] The redox behaviour of pBQ as an example is shown in **Figure 5**.

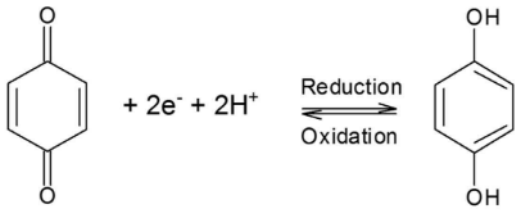

Figure 5: Scheme of the oxidation and reduction reaction of pBQ.[8]

In aqueous media, the reduction process requires one proton and one electron for each hydroxyl-group formation. Considering this, a quinone undergoes two-proton-two-electron transfer.[10] Highly important is that the number of electrons transferred determines the energy density. Therefore, quinones are of great interest for many researchers in aqueous organic RFBs due to their fast two-electron transfer in a single step.[9,10]

The chemical stability of quinones is the reason for the challenges concerning long life cycling and storage stability in RFBs. The degradation mechanisms of the active species should be studied in more detail to improve chemical stability, as this is a major factor for inefficiencies and low utilisations in organic redox couples.[10] Also, some side reactions may occur. Hydroquinones form extremely reactive superoxides and hydrogen peroxide in presence of oxygen (**Figure 6**).[8]

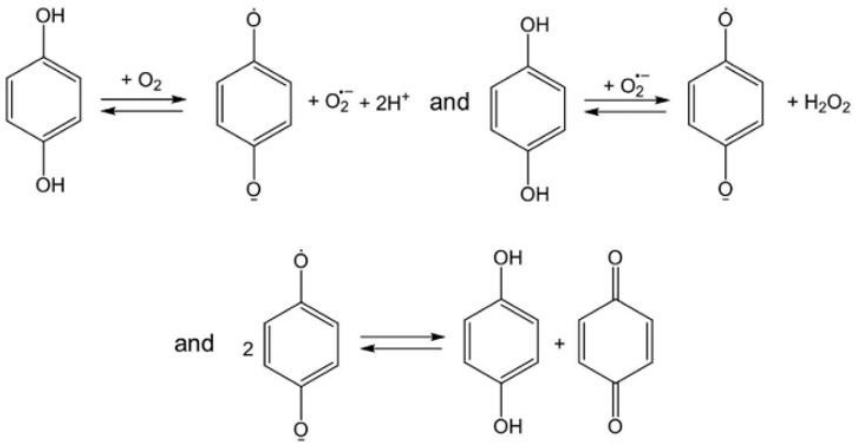

Figure 6: Superoxide and hydrogen peroxide formation with hydroquinone.[8]

Quinones are generally stable at acidic pH values, as they decompose in alkaline solutions via nucleophilic substitution and addition reactions. The limit is the poor solubility in acidic solutions which decreases the volumetric capacity of the RFB.[12] Some of the organic RFBs use conventional cell component materials (electrodes and separator), which also need to be optimised to improve the overall performance.[10]

1.1.4 Chlorogenic acid

Chlorogenic acid (CGA) is one of the main polyphenols in plant and plant-based foods e.g. coffee or tea. It is an ester consisting of quinic acid and *trans*-cinnamic acids such as caffeic acid, ferulic acid and *p*-coumaric acids.[13,14] The chemical structure is depicted in **Figure 7**. Furthermore, CGA can be hydrolysed to yield caffeic acid.[15] CGA and CA are known as antioxidant agents and are heavily used as an anti-inflammation substance.[13,14]

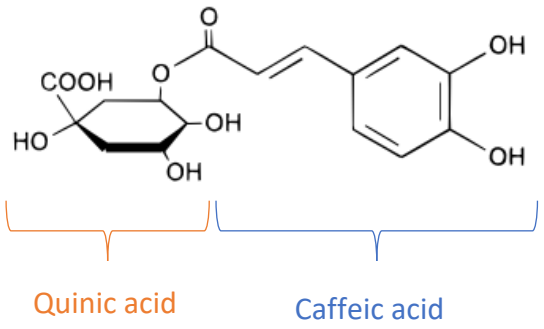

Figure 7: Chemical structure of CGA consisting of quinic acid and caffeic acid.

CGA stands for all nine hydroxyl cinnamic esters which can be found in green coffee beans namely coumaroyl quinic-, feruloyl-, caffeoyl- and dicaffeoylquinic acids (**Figure 8**). The most available CGA of all CGAs in green coffee beans is 5-CQA with an amount of 76-84%.[13]

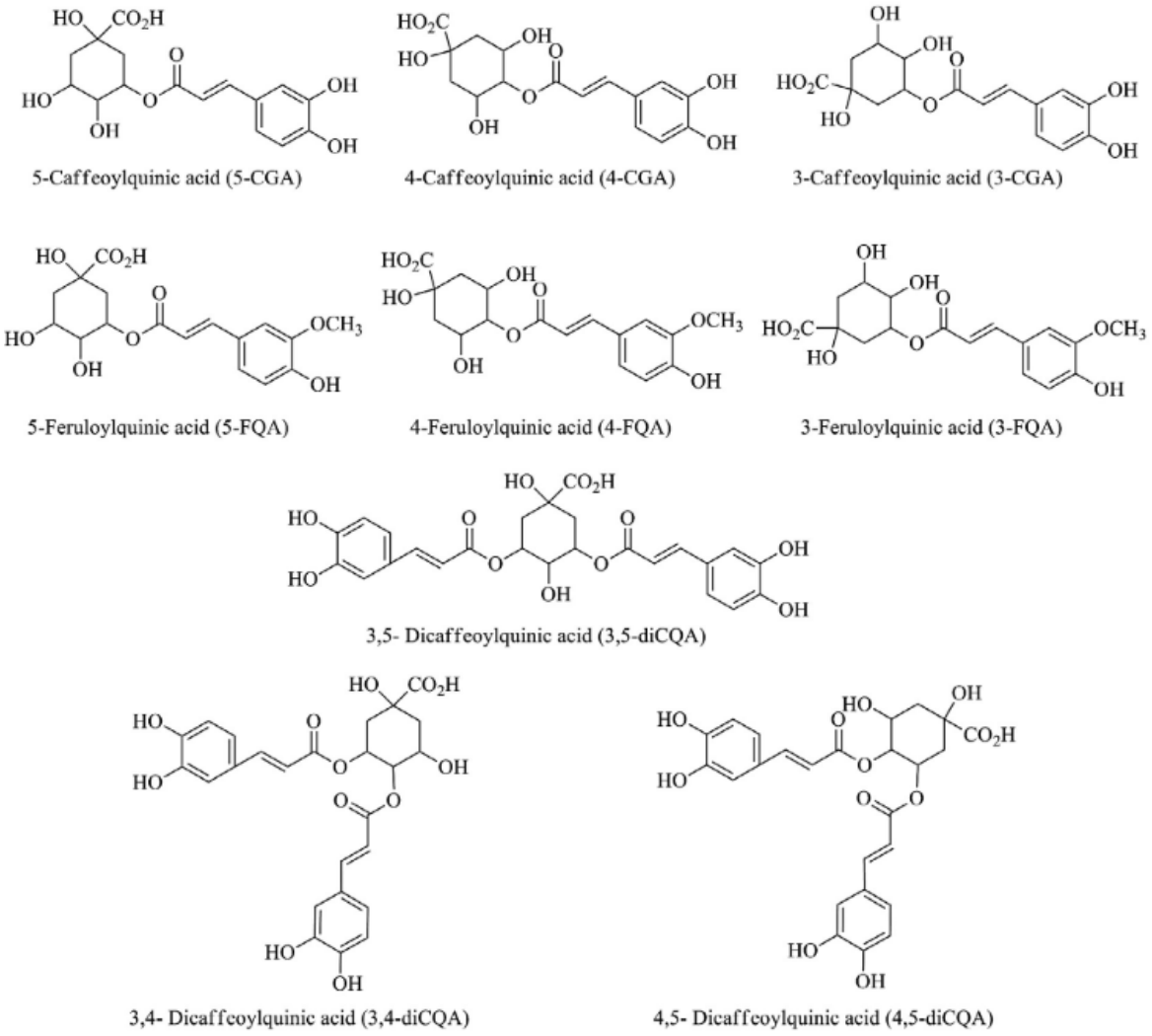

Figure 8: Structures of the main CGAs found in coffee.[16]

The industrial roasting process of the green coffee beans influences the CGA content. The content reduces about 8 – 10% for every 1% reduction in dry matter. This results in losses of 60 – 70% for medium roast and 90 – 95% for dark roast due to its thermal instability.[17,18] The different levels of roasting including the roasting time and temperature are shown in **Figure 9**. Furthermore, the organic acid content increases with increasing roasting times while the CGA content decreases.[19]

Figure 9: Coffee beans with different levels of roasting.[20]

In addition, CGA and quinic acid form chlorogenic acid lactones (CGL) during roasting by the loss of a water molecule from quinic acid under formation of an intramolecular ester bond. Seven CGLs can be found in roasted coffee beans (**Figure 10**).[14,21]

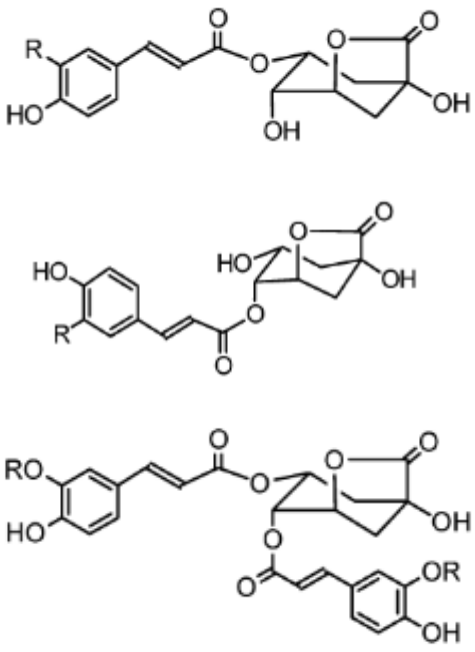

(1) 3-caffeoyl-1,5-quinide (R=OH)
(2) 3-*p*coumaroyl-1,5-quinide (R=H)
(3) 3-feroyl-1,5-quinide (R=OMe)

(4) 4-caffeoyl-1,5quinide (R=OH)
(5) 4-*p*coumaroyl-1,5-quinide (R=H)
(6) 4-feroyl-1,5-quinide (R=OMe)

(7) 3,4-dicaffeoyl-1,5-quinide (R=H)

Figure 10: Structures of the chlorogenic acid lactones (CGL) in roasted coffee.[21]

CGA and CA can both be found in coffee beans whereas numerous literature can be found for CGA[14,21–25] and less literature is known for CA content analysis.[14,26] The CGA content in green coffee beans of Arabica and Robusta is 6.7-9.2% and 7.1-12.1%, respectively. These values include mono-, dicaffeoyl- and feruloylquinic acids.[22]

1.2 Cyclic voltammetry

Cyclic voltammetry (CV) is a widespread electrochemical technique that allows investigations of the oxidation and reduction behaviour of molecules. The voltage (E) is swept linearly with a constant scan rate (v) between an upper and lower limit, giving a triangular shaped voltage sequence. The corresponding current (i) response is plotted against the voltage, this "duck" shaped plot is called a cyclic voltammogram and is depicted in **Figure 11**. The arrows indicate the scanned sweep direction, whereas the first peak shows the oxidation process and the second peak the reduction process. The scan rates used for CV measurements can vary, although common values are between 10 mV/s and 1000 mV/s.[27]

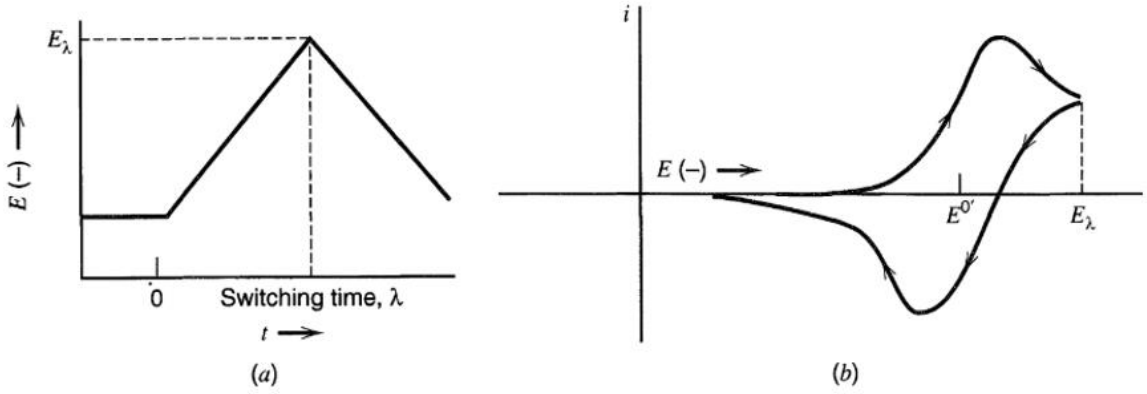

Figure 11: (a) Triangular shaped voltage sequence. (b) Cyclic voltammogram.[28]

In an ideal reversible process, the peak to peak separation (difference between the anodic and cathodic peak potentials) is 57 mV. This chemical reversibility indicates whether the dissolved redox active compound (analyte) remains stable during oxidation and subsequent reduction processes. Homogeneous processes like ligand losses or degradation are not chemically reversible. Electrochemical reversibility refers to the electron transfer kinetics. Fast scan rates lead to a decrease of the diffusion layer and higher current peak maxima are measured than at low scan rates. The peak current (i_p) increases linearly to the square root of the scan rate ($v^{1/2}$) if the electron transfer at the electrode is fast.[27] For reversible reactions, the Randles-Sevcik equation indicates whether an analyte is freely

diffusing in solution (**Equation 8**).[8] Contrary to a freely diffusing redox species, the current response is linear with the scan rate (ν).[27]

$$i_p = 0.446\,(F^3 * (RT^{-1})^{\frac{1}{2}}\, n^{\frac{3}{2}}\, A\, D^{\frac{1}{2}}\, C_O\, v^{\frac{1}{2}}$$ **Equation 8**

i_p.....Peak current [A]

F .....Faraday constant [C/mol]

R.....Gas constant [J/mol*K]

T .....Temperature [K]

n .....Number of electrons transferred []

A.....Electrode area [cm^2]

D.....Diffusion coefficient [cm^2/s]

C_O .....Concentration [mol/cm^3]

v .....Scan rate [V/s]

Typically, a three-electrode set-up is used for the CV measurement (**Figure 12**). In an electrochemical half-cell, electrons are transferred from the electrode to the analyte. The ions move in the solution to balance the charge and close the electrical circuit. To reduce the resistance in the solution, a salt is dissolved as a supporting electrolyte. Additionally, the supporting electrode increases the conductivity of the solution.[27]

A good supporting electrolyte has the following properties: It is highly soluble in the solvent, chemically and electrochemically inert in the conditions of the experiment and it can be purified. A good solvent has these properties: It is liquid at experimental temperatures, completely dissolves the redox active compound and the supporting salt, is stable during the redox processes in the chosen potential range, is inert to the analyte and the supporting salt and it can be purified.[27]

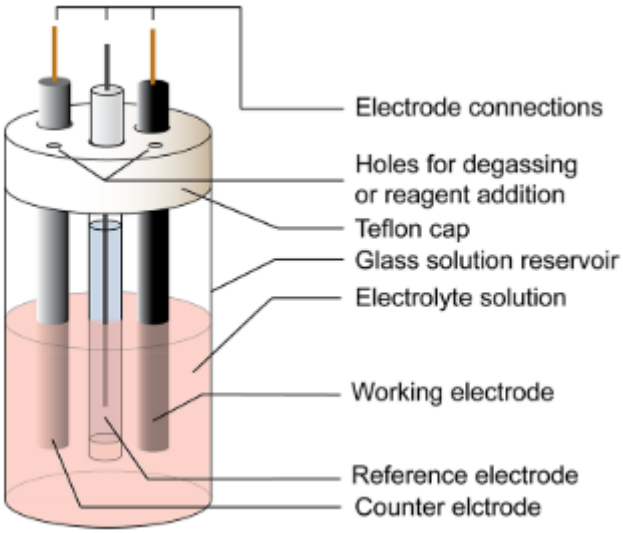

Figure 12: Assembly of an electrochemical half-cell for CV experiments.[27]

A potentiostat is used to control the applied potential. Usually, a glassy carbon working electrode (WE) is used. During the reduction at the WE, the oxidation is carried out at the counter electrode (CE), therefore the CE should be as inert as possible. A platinum wire or disk is typically used. The reference electrode (RE) accurately measures the applied potential relative to a stable reference reaction. Commonly used RE's are the saturated calomel electrode (SCE), the standard hydrogen electrode (SHE) and the Ag^+/Ag electrode.

1.2.1 Pourbaix diagram

Pourbaix diagrams or the so-called potential pH diagrams were developed by Marcel Pourbaix in 1938. The diagram shows the pH dependence of electrochemical stability for different redox states of metals. It represents the ranges of thermodynamic stability in metal-electrolyte systems and is used to predict whether or not a metal might corrode. The redox potential is on the vertical axis and the pH-value is on the horizontal axis.[29]

In the case of quinones, the redox potential (E^0) highly depends on the pH value as depicted in **Figure 13**. This scheme was made using two anthraquinone derivatives that have the same pK_a values. Horizontal movement indicates electron transfer and vertical indicates proton transfer. In areas between the tested pH values, several paths are possible at the

same time. It is also worth mentioning that the redox reactions are not always the same, as there is the possibility that the rate-determining electron transfer step changes with the potential. At a pH value of 1, the reaction includes two protons and therefore the redox potential (E^0) decreases with 59 mV/pH unit. At alkaline pH values, E^0 decreases with 30 and 0 mV/pH unit as only one or no protons being concerned, respectively.[8,30]

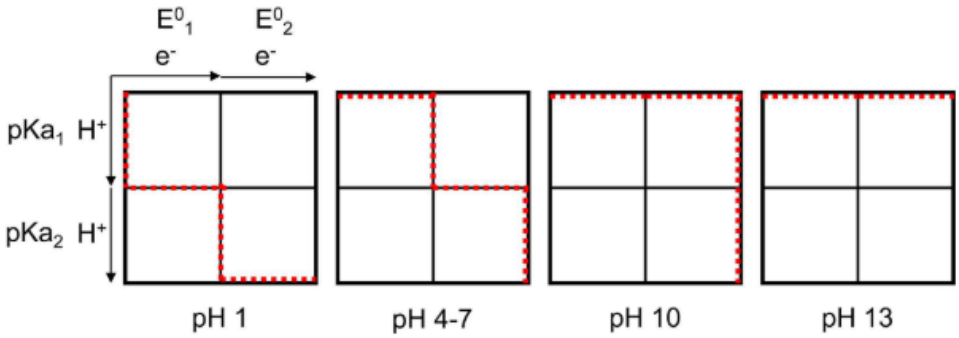

Figure 13: Scheme-of-squares for anthraquinone-2,6-disulfonate and anthraquinone.[8]

1.3 Coffee

Coffee is one of the most popular brewed beverages worldwide. More than 70 countries produce coffee, primarily in the equatorial region (**Figure 14**). The global production leader is Brazil, followed by Vietnam, Indonesia, Colombia and India while the top leading coffee importers are the USA, Germany, Italy, Japan and Belgium. Regarding coffee production, 60 percent is Arabica (*Coffea Arabica*) and 40 percent is Robusta (*Coffea Canephora*). Not only is coffee produced in large quantities, it also comes in a wide variety of qualities, types and forms, for example roasted, green or instant. In many of these developing countries, coffee exports are the most important sources of income.[31]

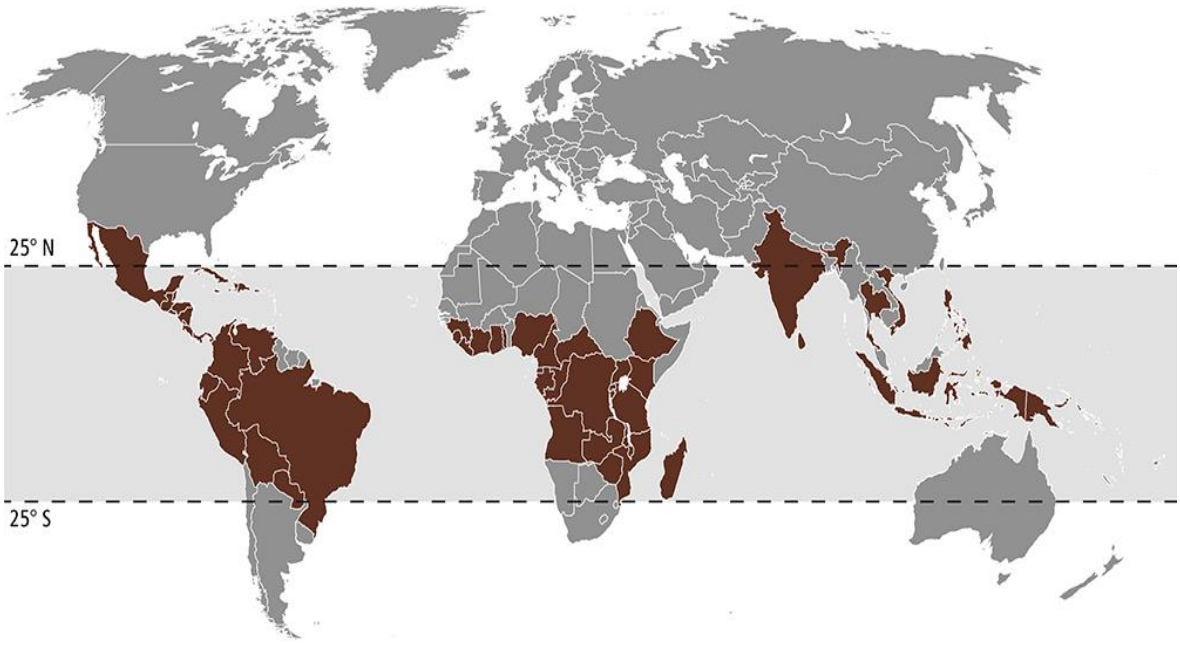

Figure 14: Coffee growing areas as known as "Bean Belt".[32]

The International Coffee organisation stated that the global exports had increased by 5.7% compared to the previous year, reaching 10.15 million bags only in November 2020. The Arabica exports totalled 79.81 million bags in the latest coffee year, whereas Robusta exports reached 48.66 million bags. In December 2020, the total coffee price increased by 8% to 114.96 US cents/lb for Brazilian Naturals for Arabica. The prices for Colombian Milds (5.7% to 170.44 US cents/lb) and other Milds (4.7% to 157.81 US cents/lb) has also increased. The prices for Robusta fell by 0.5% to 72.04 US cents/lb.[33]

1.3.1 Coffee industry by-products and their composition

The green coffee bean is covered by the coffee silver skin (CSS), an endcarp (parchment), a pectic adhesive layer, pulp and the epicarp (outer skin) as displayed in **Figure 15**.[34] The green coffee bean consists of 50 wt% of the coffee cherry, while the pulp and skin (41 w%), outer skin (7-8 wt%) and CSS (1.2 wt%) make up the rest.[35]

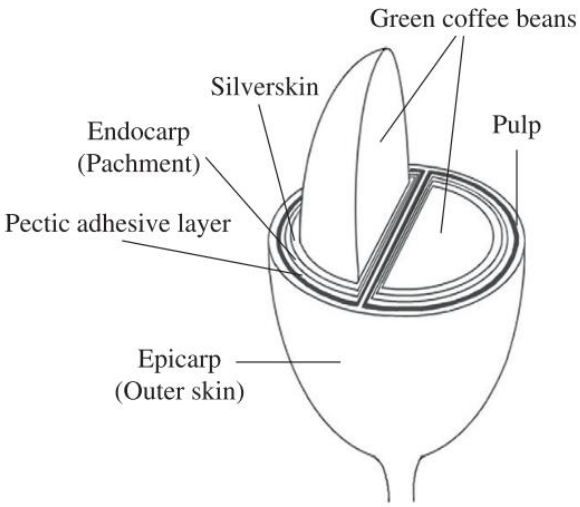

Figure 15: Structure of the coffee cherry.[34]

The purification of the green beans is either done by the dry or wet method. The dry method yields the husk and is mainly used for Robusta, while the wet method is generally used for Arabica and yields pulp. These methods remove the outer skin, pulp and husk. CSS is the only by-product of the following roasting process of the green beans.[35] A visualisation is given in **Figure 16**.[36]

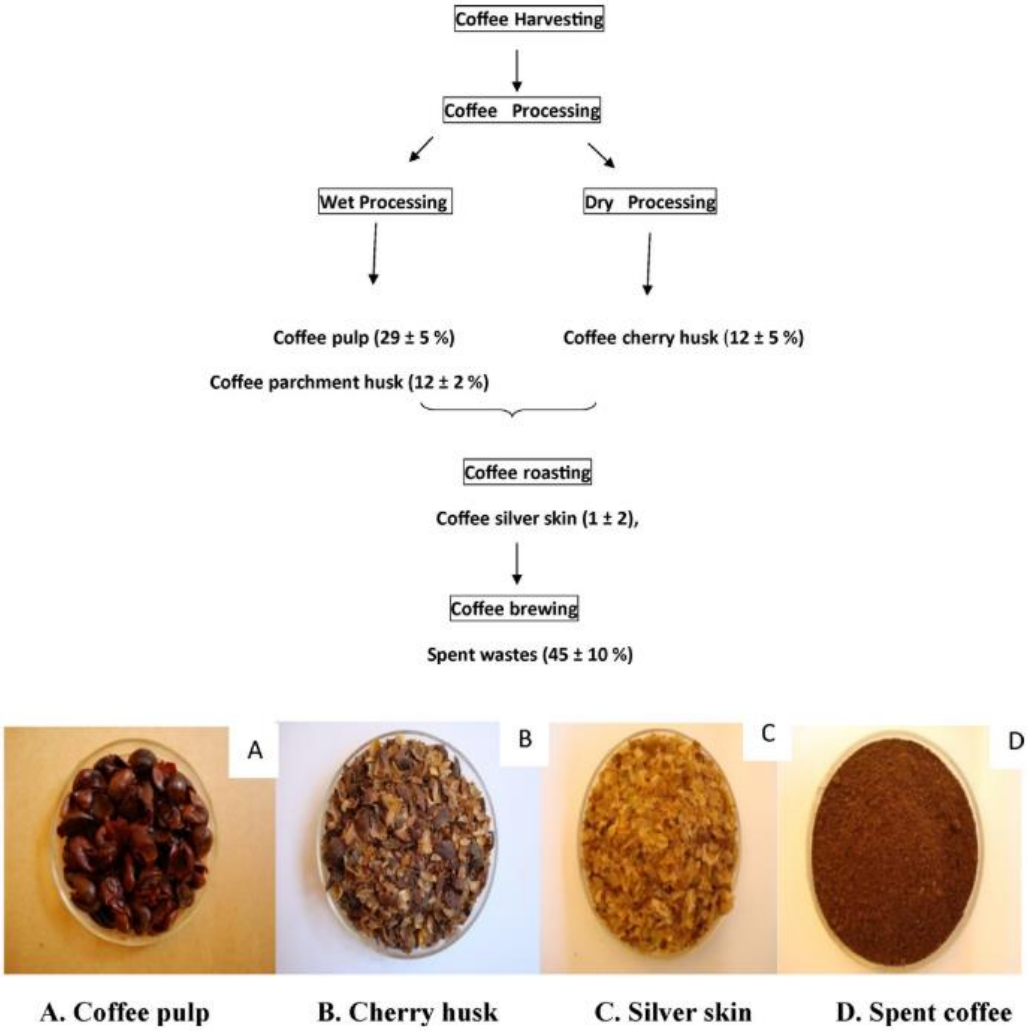

Figure 16: Formation of by-products from coffee industry with images of these by-products.[36]

All steps of the industrial coffee process, from beans production to coffee brewing, produce a large amount of waste. For every tonne of fresh coffee, 0.5 and 0.18 tonnes of coffee pulp and husk are produced. About six million tonnes of spent coffee grounds (SCG) are produced worldwide each year, with one tonne of green coffee yielding 0.65 tonnes of SCG.[35] About nine million tonnes of spent coffee grounds were dumped in landfills. The formation of coffee waste is shown in the life cycle of coffee as depicted in **Figure 17**.[37]

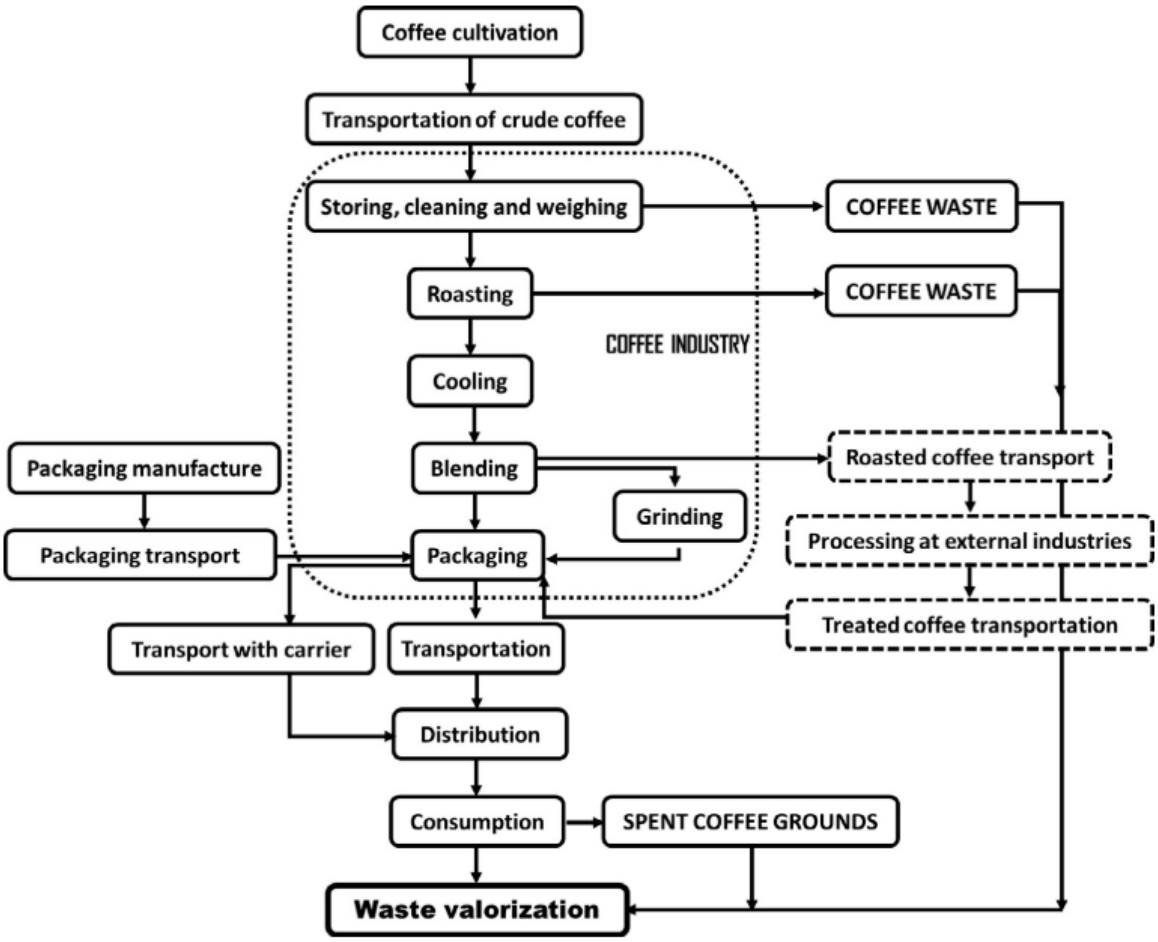

Figure 17: Live cycle assessment of coffee.[37]

The composition of the green coffee beans of Arabica and Robusta according to Belitz et al.[22] is 9-12.5% and 6-11.5% soluble carbohydrates, 46-53% and 34-44% insoluble polysaccharides, 41-43% and 32-40% cellulose, 6.7-9.2% and 7.1-12.1% chlorogenic acid, 15-18% and 8-12% lipids and 0.8-1.4% and 1.7-4.0% caffeine, respectively.

SCG consist of 53 w% carbohydrates (whereas 8.8% is cellulose and 44.5% is hemicellulose), 12.6 w% lipids, 13.8 w% protein and 13.1 w% insoluble lignin.[15] In addition, CSS consist of 52.1% carbohydrates, 53.7% insoluble dietary fibre, 53,7% soluble dietary fibre, 18.6% proteins and 2.2% fats.[34]

The most important factor is that the composition depends on variety, growth region, growth behaviour, climate and the processing. The processing step includes harvesting time, purification, roasting, storage and packaging.[18,22]

1.3.2 Industrial application of coffee waste

Due to the high volume of waste generated during industrial coffee processing, many researchers are focusing on the recycling of coffee waste. The sustainable usage of natural sources helps to reduce environmental pollution. Previously, the applications were inefficient or technically immature and included processes such as animal feed, composting and fertilisers. These applications are now being optimised and continuously developed. Applications are mushroom cultivation, the production of enzymes, organic acids, biofuels and fertilisers.[35]

Bioactive compounds such as phenolics occur in high amounts in coffee by-products. They are obtained by solid-liquid extraction. Phenolic acids raise ecotoxicological concerns, such as chlorogenic acid, which has phytotoxic properties. However, phenolic compounds limit the usage of coffee husk and pulp for bioprocesses and composting. Composting is a low-cost solution of agricultural-industrial waste treatment, which results in nutrimental fertilisers. SCG and CSS are well suited for dietary fibre and enzyme production. Since the total waste of SCG and CSS is about 50% they are ideal for fertiliser production. But the problem is the missing infrastructure for this large supply.[35]

1.3.3 Coffee biorefinery

The oldest and most commonly used method for coffee extraction is the liquid-solid extraction with a Soxhlet apparatus.[37,38] Further techniques are shaking or sonication. Especially, sonication can gently heat the samples if a bath is used and the speed of this extraction allows multiple extractions in a short time (approximately 3 min per extraction).[38]

Also, conventional and supercritical-extractions are widely used to e.g. extract oil from coffee samples. For conventional extraction the sample is mixed with a solvent and stirred. Then the solid has to be separated from the extract. However, this is less effective than a Soxhlet extraction. Supercritical-extractions replace harmful volatile solvents which are

necessary for extracting oil. Supercritical carbon dioxide is used as a more environmentally friendly solvent. Its properties can be changed by changing pressure and temperature.[37]

In general, Soxhlet extraction is the method of choice due to its simplicity. It continuously recirculates the solvent through the sample. This saves solvent and allow a maximum output.[39]

2 Research objective

The main objective of this work is to fully extract the desired quinones (CGA and CA) in coffee samples with inexpensive solvent mixtures. In addition, their redox activity for RFB testing should be confirmed.

To determine the yields of CGA and CA, thin layer chromatography and gas chromatography coupled with mass spectroscopy were used. Cyclic voltammetry and a redox flow battery cell were applied for electrochemical measurements.

This research has the following steps:

- Extraction of coffee samples
- Development of TLC analysis
- Comparison of TLC analysis with GC-MS measurements
- Investigating whether pBQ, CA and CGA are suitable materials for RFBs by cyclic voltammetry measurements
- Redox flow battery testing

In addition, this work should find more environmentally friendly replacements for harmful substances.

3 Experimental

3.1 Materials and methods

3.1.1 Chemicals

Chlorogenic acid (98%, predominantly trans, from coffee seeds) was obtained from ACROS Organics and caffeic acid (98%, predominantly trans) was purchased from Alfa Aesar. *Para*-benzoquinone (≥ 98%), sodium phosphate dibasic dihydrate (≥ 99%) and Tween®80 (cmc = 0.012 mM in water at 20 – 25 °C) were acquired from Sigma Aldrich. Citric acid (≥ 99%, anhydrous) was from Merck and potassium chloride (< 99%) was acquired from Fluka.

Isopropanol (≥ 98%), 2-butanone (≥ 99.5%), *ortho*-phosphoric acid (85%) and pyridine (≥ 99%) were obtained from Carl Roth GmbH. Ethanol (≥ 96%) and hydrochloric acid (37%) were purchased from VWR International GmbH. Formic acid (98-100%) from Merck and ethyl acetate (99.98%) from Fluka were used as solvents.

Hydrogen peroxide (30%) from Carl Roth GmbH and sulfuric acid (95%) from VWR International GmbH were used for the activation of the electrodes and membranes, respectively. For the GC-MS (gas chromatography coupled with mass spectroscopy) sample preparation *N,O*-bis(trimethylsilyl)trifluoroacetamide (99%, with 1% trimethylchlorosilane) (BSTFA-TMCS) was obtained from Alfa Aesar. All chemicals were used without further purification.

3.1.2 Plant materials

Spent coffee grounds, coffee silver skins, green beans (*Coffea Arabica*), roasted beans (*Coffea Arabica*), cocoa shells, abrased coffee and instant coffee (Spar: REGIO - Caffè Crema Löskaffee) were supplied by Dieter Wurm. Prior to the experiments, green and roasted beans were milled with a Delonghi KG49 at the highest power level. The samples were stored under a constant climate with a moisture content of 50 ± 2% at 23 ± 2 °C for 48 h until further usage. This condition was in accordance with ISO 187, which is the standard test climate for measuring paper properties.

3.1.3 Dry content determination

The dry weight of the given samples was determined by weighing an amount of sample (5 g) and heating it at 105 ± 2 °C for 48 h according to ISO 287:2017. The dry weight was determined gravimetrically by double determination.

3.1.4 Ash content determination

The samples were weighed and incinerated in a muffle furnace at 575 °C for 24 h. They were consequently weighed again and the ash content was calculated.

3.1.5 Soxhlet extraction

5 g of a sample were extracted using a 500 mL round neck flask and 150 mL of solvent mixtures (ethanol:water (3:2, v:v) and isopropanol:water (3:2, v:v), respectively). Spent coffee grounds, coffee silver skins and cocoa shells were extracted for a duration of 4.5 h and green beans, roasted beans, abrased coffee and instant coffee for 8.5 h due to the latter containing more CGA and requiring a higher extraction time. The first 0.5 h are needed until the Soxhlet apparatus is running constantly. The extracts were allowed to cool down to room temperature and diluted with dist. water to 250 mL in order to have a defined volume for TLC analysis. All extracts were stored in the refrigerator (8 °C) until further usage. All experiments were done by triple determination.

3.1.6 Thin layer chromatography (TLC)

HPTLC silica gel 60 F_{254} plates on aluminium support from Merck and glass ringcap capillaries with a defined outlet volume of 10 µL from Hirschmann were used. The TLC development chamber has an inner dimension of 8 x 3 cm. A mixture of ethyl acetate:2-butanone:formic acid (3:2:0.025, v:v:v) was used as eluent (CGA (R_f: 0.17), CA (R_f: 0.79)). Then, the plates were left to dry in the air and the visualisation was carried out under short UV wavelength (254 nm) and photos of the plates were taken for the quantitative evaluation. In addition, a reference with 5 µg CGA and CA each was spotted.

3.1.7 Camera and graphical image evaluation

All photos of the TLC plates were taken using a Samsung Galaxy A3 smartphone with a 13-megapixel camera. The optical image evaluation was carried out using the Fiji software, which is a distribution of ImageJ and is open source.[40] The evaluation was as followed:

1. Open a photo file
2. Click on 'Image', 'Color' then 'Split channel'
3. Keep the 'green' named window
4. Mark the spots on the TLC image with the 'Rectangle' tool
5. Click on 'Analyze', 'Gels' and 'Select First Lane'
6. Click on 'Analyze', 'Gels' and 'Plot Lanes'
7. Draw the baseline with the 'Straight' tool
8. Click 'Analyze', 'Measure' and delete the value there
9. Use the 'Wand' tool on the peak areas to integrate them
10. Click 'Analyze', 'Gels' and 'Lable Peaks' to show the percentages

3.1.8 Gas chromatography-mass spectrometry (GC-MS)

Prior to the measurement, a certain volume of each extract was evaporated to adjust the mass to the appropriate range of the GC-MS system (5 - 20 mg analyte dry mass per sample). The dried samples were stored in the freezer until further usage.

The samples were dissolved in 1 mL pyridine and were silanized using 100 µL N,O-bis(trimethylsilyl)trifluoroacetamide (99%, with 1% trimethylchlorosilane).[12] The measurements were carried out with a SHIMADZU GC-MS QP2010 Plus GC-MS system, equipped with a fused silica capillary column (Optima-5-Accent-30 m × 0.25 mm × 0.25 µm film thickness), an AOC-20i automatic sampler, a split/splitless injector and a mass selective detector. The injection temperature was kept at 280 °C. The oven temperature program was set from 60 °C to 200 °C with a heating rate of 10 °C/min and from 200 °C to 280 °C with a heating rate of 3 °C/min. The mass spectra recorded were in a m/z range of 35 - 600.

3.1.9 Solubility testing of caffeic acid

A stock solution of 4 mg CA in 10 mL solvent was prepared, which was then diluted to the desired concentrations. The used solvents were dist. H_2O and 0.5 M H_3PO_4, each with and without Tween®80 (0.5 wt%) as surfactant. In addition, blank and saturated samples were investigated. The solutions were dissolved via an ultrasonic bath, left to equilibrate for 30 minutes and investigated afterwards. The solubility test of the CA was carried out with an Anton Paar Abbemat 550 Refractometer. For this, some drops of the prepared solutions were placed onto the prism, the apparatus was closed and the refractive index was determined.

3.1.10 Buffer preparation

1 M citric acid and 2 M sodium phosphate dibasic dihydrate were used. The pH values of the buffer were 2.6, 2.8, 3.0, 3.2, 3.4, 4.0 and 4.5, respectively. This can be calculated according to the Henderson-Hasselbalch-equation (**Equation 9**).

$$pH = pK_s - log_{10} \frac{c\,(A^-)}{c\,(HA)} \qquad \textbf{Equation 9}$$

3.1.11 Cyclic Voltammetry

The cyclic voltammetry measurements were carried out using an Arbin LBT potentiostat with the MITS Pro software from Arbin Instruments (Texas, USA). The samples were investigated using a tree-electrode set-up as mentioned in 1.3. The electrodes were a GCE glassy carbon electrode with a diameter of 1.6 mm (working electrode), a MW 4130 Platinum Wire Auxillary Electrode (counter electrode) and a Ag/AgCl Reference Electrode (E_0=195 mV vs. SHE) from ALS Co., Ltd. The potential range for the voltammograms was -1 to +1 V. In addition, KCl was added to all measurements as a supporting electrolyte. The used weights are listed in **Table 1**.

Table 1: Sample weights for the CV measurements.

H_3PO_4	pBQ [mg]	CA [mg]	CGA [mg]
0.01 M	0.54	0.51	1.06
0.05 M	0.53	0.57	1.00
0.1 M	0.53	0.61	1.08
0.5 M	0.52	0.53	1.06
1 M	0.50	0.60	1.06
buffer (1M, 2M)			
pH = 2.6	0.49	0.51	1.06
pH = 2.8	0.52	0.54	0.99
pH = 3.0	0.49	0.53	1.03
pH = 3.2	0.56	0.51	1.02
pH = 3.4	0.50	0.49	1.05
pH = 4.0	0.51	0.53	1.02
pH = 4.5	0.52	0.53	1.08

3.1.12 Redox flow battery assembly

The test cell was a LAB-1×1 from C-Tech Innovation Ltd. (Chester, UK) with 1 mL active volume per compartment and PTFE tubing. The solutions were kept in polypropylene storage tanks and guided through the flow cell by a self-made pumping system with 150 mL/s flow (**Figure 18**). In order to achieve a homogeneous flow an Arduino Uno ATmega328 microcontroller, a Recom LED driver, an LCD display, RS pro flow sensors (0.05 – 10 L/min), a mean well power adapter (32 W, 6 A), a Fibox Euronorm cask, a MH Connector Sub-D, and a RS Pro Sub-D Print connector form RS Components (Gmünd, Austria) were utilised to control two WPDC-0.45L-3.1M-12 rotary pumps purchased from Rotek Handels GmbH (Hagenbrunn, Austria). The redox flow battery measurements were carried out using the same potentiostat as described in 3.2.9.

AvCarb G100 Soft Graphite Battery Felt electrodes were acquired from Fuel Cell Store. The electrode was activated with Caro's acid by mixing 95% H_2SO_4 with 30% H_2O_2 3:1 (v:v) for 10 minutes at room temperature. Then it was stored in 0.5 M H_3PO_4 until usage.

A Nafion NR 211 membrane with a thickness of 25.7 µm from Fuel Cell Store (College Station, USA) was acquired. The membrane was conditioned using H_2O_2 (3%) at 90 °C for 1 h and it was stored in 0.5 M H_3PO_4.

The half-cells were operated potentiostatically with 7.5 mg CA (anolyte) and 5 mg pBQ (catholyte) as active materials in 35 mL of 0.5 M H_3PO_4 each. The flow rate was 150 mL/s, the charging/discharging time was 1.5 h at constant potentials of +0.75 V and -0.75 V, respectively.

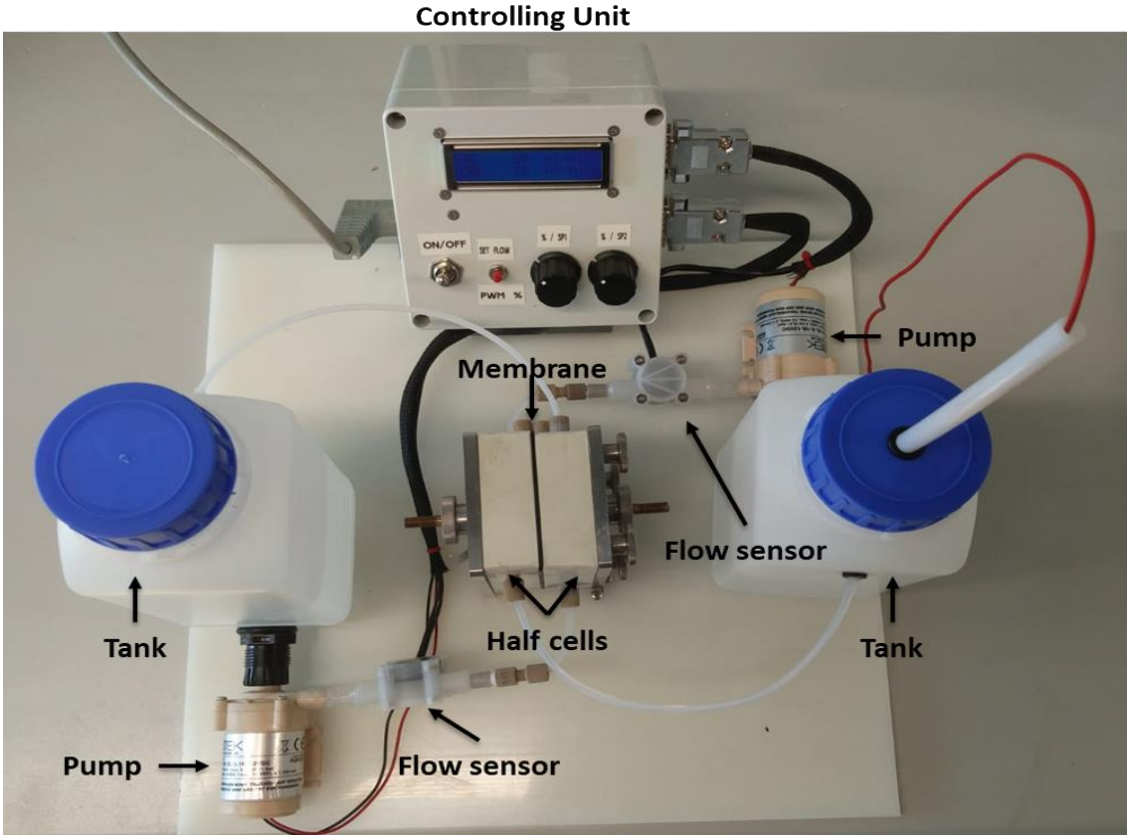

Figure 18: Set up of the redox flow battery.

4 Results and discussion

4.1 Dry matter and ash content of the samples

Determination of dry matter is important because high moisture content leads to sample corruption and microbial growth.[34] Therefore, the samples would mould and no longer be usable.

The measured moisture content in green beans was 8.9% (**Table 2**). The International Coffee Council demands a moisture content of 8.0-12.5% for green beans.[41] The experimentally determined value agrees with this. In literature, a moisture content of 10-12% is given for green beans.[42] The moisture drops to approximately 5%[42] after roasting which corresponds to the measured data of 6.2% for roasted beans. Instant coffee results in a moisture content of 9.8%. This is higher than the literature value of about 5%[42] and might be due to the higher humidity during storing.

Table 2: Sample name and their corresponding moisture and ash content.

Sample	Dry matter [%]	Moisture [%]	Ash [%]
spent coffee grounds	91.8	8.2	1.97
coffee silver skins	90.4	9.6	7.45
green beans	91.1	8.9	4.27
roasted beans	93.8	6.2	5.16
cocoa shells	92.6	7.4	6.58
abrased coffee	93.5	6.5	5.59
instant coffee	90.2	9.8	14.1

The dry matter content was further used for the calculation of CGA and CA content. The ash content is an index for the mineral content in a sample. The major mineral elements in ground coffee beans are calcium, iron, magnesium, potassium, sodium, strontium, zinc and phosphorus.[43] In literature, spent coffee grounds, coffee silver skins, green beans, roasted beans, cocoa shells, and instant coffee have an ash content of 1.8[44], 7.0[45], 3.0-4.5[42], 6.2[44], 7.1[46] and 9-10%[42], respectively. No literature value for abrased coffee was found. A reason for the higher ash content of instant coffee (14.1%) could be the difference in the

composition of the powder of the different brands or that companies use different additives.

4.2 Extraction of the samples

4.2.1 Solvent selection

The desired redox active compounds were CGA and CA. CGA is soluble in water, alcohol and acetone[47] and CA is soluble in ethanol, water, ethyl acetate, chloroform and methanol[48] according to their supplier. Ji et al. (2016)[49] tested the solubility of CA in various solvents and stated that ethanol and isopropanol were suitable solvents. Also, various researchers had successfully extracted their coffee samples with water and alcohol-water mixtures, which are summarised in chapter 4.3.3. (**Table 5-6**). Therefore, the chosen solvent mixtures were EtOH:H_2O (3:2, v:v)[50] and isopropanol:H_2O (3:2, v:v)[24]. Ethanol and isopropanol can both be produced inexpensively using renewable resources e.g. biomass.[51] This makes them suitable for industrial applications.

4.2.2 Thin layer chromatography (TLC)

Thin layer chromatography was used as a fast and inexpensive method to analyse the extracts for their chlorogenic and caffeic acid content. The development of a suitable eluent was carried out by Melissa Egger as part of her bachelor thesis (2019). The chosen eluent was a mixture of ethyl acetate:2-butanone:formic acid (EA:B:FA) (3:2:0.025, v:v:v). Already a drop of formic acid prevents the dragging of applied analyte on the TLC plate.

A similar eluent mixture for CGA and CA was reported previously by Kanokwan et al. (2016).[52] They used toluene:ethyl acetate:water:formic acid (15:90:5:5), which makes the eluent toxic due to the utilisation of toluene. The used eluent in this work provides a greener alternative.

Calibration:

In order to evaluate the amount of CGA and CA, a calibration was set up. The spotting solvent was EtOH and the solution was further diluted to the desired concentrations. The spotted amounts were 1, 5, 10 and 20 µg. The corresponding TLC plate is shown in **Figure 19**. At this point it shall be mentioned that it was quite difficult to achieve uniform spots on the TLC plate during the spotting process. It is important to leave space between the applied areas to avoid overlapping spots. The capillary was applied several times to the same spotting area and drying pauses were taken to avoid large sized spots. The aim was to create spots that were as small as possible. Heat should be avoided as it can change the applied sample. An automatic TLC spotter would decrease operator-based deviations.

Then, the retention factor (R_f value) was calculated according to **Equation 10**. This factor is characteristic for a substance with a specific eluent. This value is the ratio of the travelled distance of the substance to the travelled distance of the eluent.

$$R_f = \frac{distance\ traveled\ by\ substance}{distance\ traveled\ by\ solvent} \qquad \textbf{Equation 10}$$

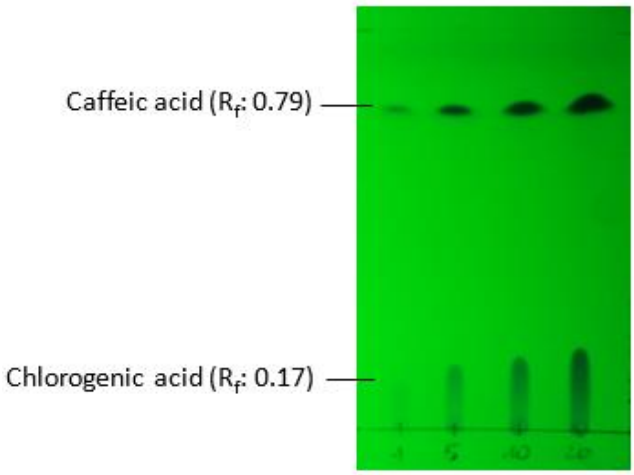

Figure 19: TLC plate of the calibration curve with masses of 1, 5, 10 and 20 µg (left to right) CGA and CA, respectively. The corresponding moles for CGA and CA were 5.6 and 2.8, 27.8 and 14.1, 55.5 and 28.2, and 111.0 and 56.4 nmole, respectively. The eluent was EA:B:FA (3:2:0.0025, v:v:v). The visualisation was carried out under UV-wavelength (254 nm). The spots were CGA (R_f: 0.17) and CA (R_f: 0.79).

The image of the TLC plate was evaluated with an image analysis program (Fiji). The evaluation was carried out according to the procedure described in chapter 3.1.6. The integration of the converted peak areas gives the area percentages, which were then plotted against the mass. The higher the concentration of the substance, the darker and larger the spots appear on the TLC plate. This indicates a linear dependence (**Figure 20**). CGA shows a regression (R^2) of 0.999 whereas CA has a R^2 of 0.9502. Both regressions demonstrate a high accuracy that can be achieved with this simple method.

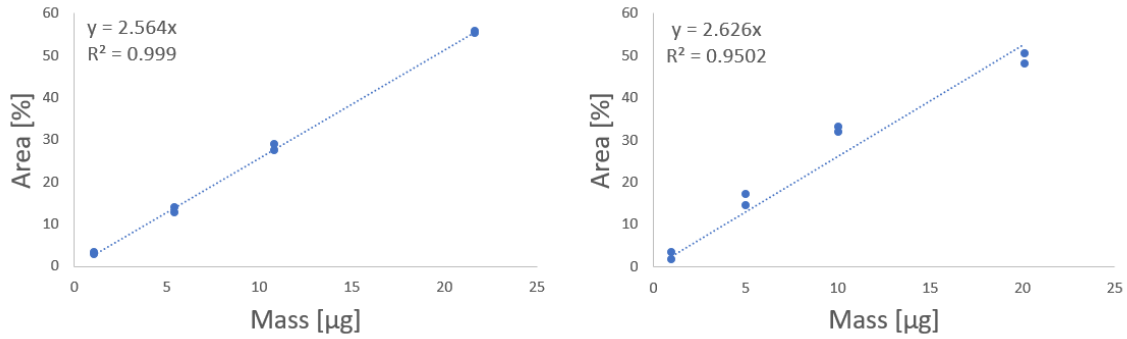

Figure 20: TLC calibration of CGA (left) and CA (right).

4.2.3 Extraction trials

The goal was to obtain high yields of CGA and CA from the samples in order to use them as redox active materials. Therefore, the extraction time of the samples with a lower expected CGA and CA content, namely spent coffee grounds, silver skins and cocoa shells was set to 4.5 h. The others were extracted for 8.5 h, as **Figure 21** reveals, so that the desired phenolic compounds are still present in the second round of extraction. Therefore, more than 4.5 h are needed for the full extraction.

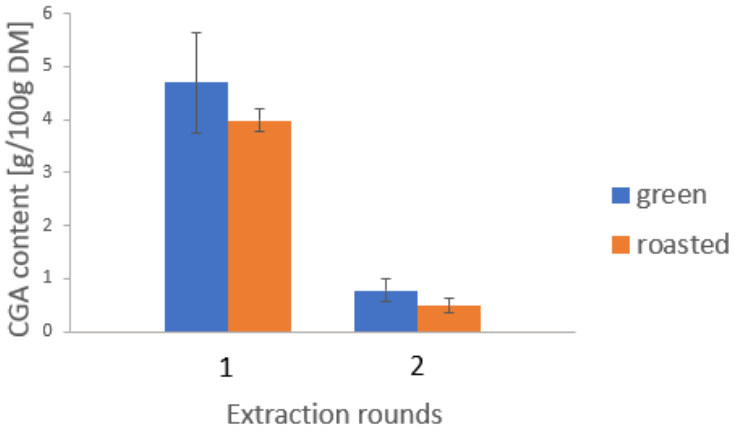

Figure 21: CGA content analysis with TLC of green and roasted beans extract with EtOH:water (3:2). The samples were extracted two times for 4.5 h to show that a higher extraction time is needed for these samples.

The corresponding masses of the extracts are listed in **Table 3**. Concerning the standard deviation, there are no mass differences between the selected solvent mixtures. This leads to the first assumption that there are no differences between the solvent mixtures.

Table 3: Average crude mass of 5 g of the extracted materials. A triple determination was carried out. SD means standard deviation.

Source	EtOH:water (3:2)		Isopropanol:water (3:2)	
	Mass [g]	± SD [g]	Mass [g]	± SD [g]
spent coffee grounds	0.69	0.08	0.66	0.06
silver skins	0.74	0.11	0.54	0.07
green beans	1.17	0.22	0.99	0.14
roasted beans	1.27	0.07	1.15	0.24
cocoa shells	0.61	0.07	0.62	0.06
abrased coffee	0.95	0.11	0.88	0.11
instant coffee	3.18	0.26	2.16	0.45

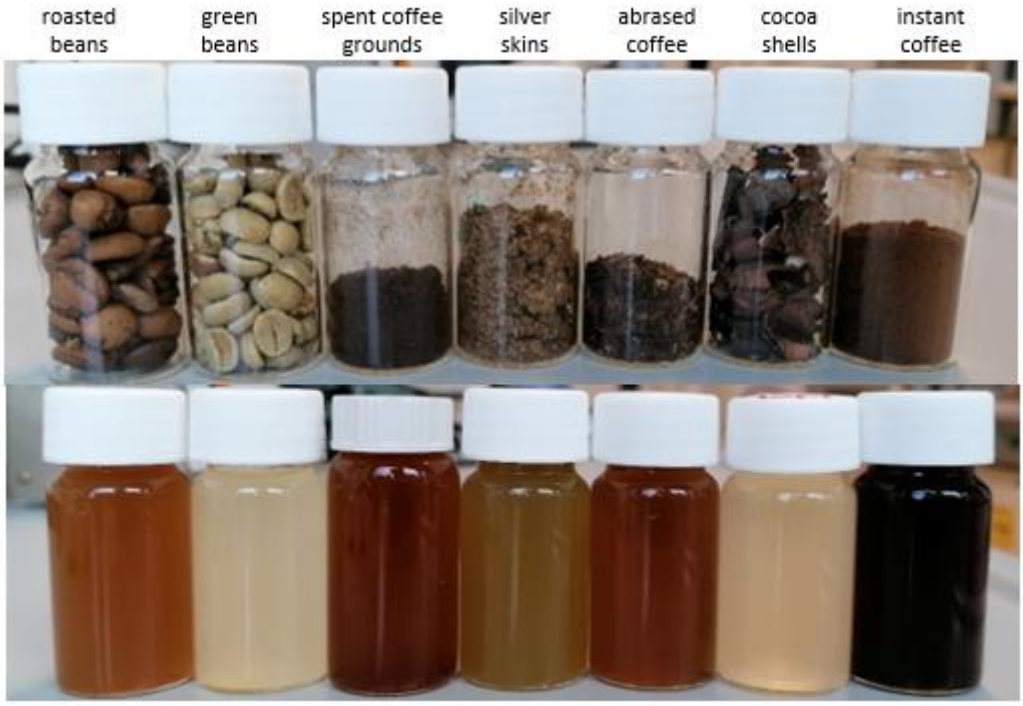

Figure 22: Photographs of the untreated samples (top) and their corresponding EtOH:water (3:2) extracts (bottom).

A comparison of the untreated samples and their corresponding extracts is shown in **Figure 22**. The green coffee beans extract was originally rather green and the cocoa shells extract was more of a yellowish colour. This was caused by dilution with dist. water to obtain a defined volume for TLC analysis.

The extracts were then analysed by TLC and GC-MS.

4.2.4 Analysis of the extracts

An example of the irradiated TLC plate of spent coffee grounds extracted with EtOH:water (3:2, v:v) is depicted in **Figure 23**. A reference (R) of 5 µg CGA and CA per spot was included, respectively. The reason for the slightly changed R_f-value compared to the one for the calibration might be due to the small amount of FA used for the eluent. It equals a volume of a droplet, which is not always the same size. However, it is not of importance as there is always a reference spot.

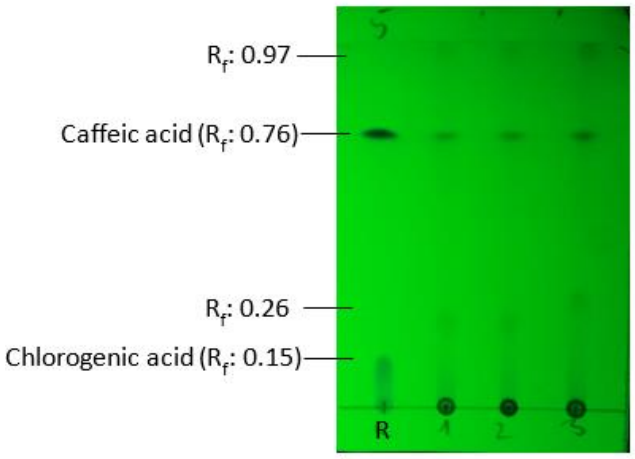

Figure 23: TLC plate of spent coffee grounds extracted with EtOH:water (3:2, v:v). The eluent was EA:B:FA (3:2:0.0025, v:v:v). The visualisation was carried out under UV-wavelength (254 nm). The spots were CGA (R_f: 0.15) and CA (R_f: 0.76).

With the reference spot, CGA (R_f: 0.15) and CA (R_f: 0.76) could be determined on the TLC plate. However, there are also other spots. The spot with the R_f value of 0.97 might be triglycerides. The other spot (R_f: 0.26) is unknown, but the compound should have a polarity between CGA and CA.

By means of the linear equations obtained from the calibration, the mass of CA and CGA in the samples could be calculated. This value was corrected by the known weight of a reference (5 µg CGA and CA, respectively). After further calculations and conversions using the weight of the sample and the total volume of the gained extract, the yield of the desired compounds was determined. With the experimentally obtained dry contents, corrected yields could be determined (**Table 4**). The unit of g/100 g equals mass percentage.

Table 4: CA and CGA results of the TLC analysis.

Source	Caffeic acid				Chlorogenic acid			
	EtOH:water (3:2)		Isopropanol:water (3:2)		EtOH:water (3:2)		Isopropanol:water (3:2)	
	[g/100 g DM]	± SD	[g/100 g DM]	± SD	[g/100 g DM]	± SD	[g/100 g DM]	± SD
spent coffee grounds	1.06	0.12	1.11	0.11	1.13	0.11	1.09	0.05
coffee silver skins	0.59	0.06	0.58	0.05	0.70	0.15	0.54	0.06
green beans	0.11	0.01	0.31	0.04	4.98	0.40	3.80	0.38
roasted beans	0.77	0.03	0.56	0.03	4.46	0.24	3.13	0.21
cocoa shells	0.15	0.00	0.10	0.01	0.37	0.11	0.33	0.06
abrased coffee	0.70	0.05	0.59	0.03	2.45	0.27	1.89	0.25
instant coffee	1.61	0.12	1.36	0.01	4.75	0.30	4.21	0.33

A graphical visualisation of the results is shown in **Figure 24-25**. The results vary slightly depending on the solvent mixtures used. The extraction with ethanol:water (3:2) revealed higher CGA and CA content than isopropanol:water (3:2). The reason is the higher polarity of ethanol compared to isopropanol. In general, when mixed with water, these alcohols offer good solubility for CA (good solubility in alcohols[48]) as well as for CGA (good solubility in water[47]). In Soxhlet extraction, fresh solvent is repeatedly evaporated, condenses and drips onto the solid to extract the desired compounds. This saves solvent and allows the unit to run continuously, resulting in maximum output.

As expected, the highest CGA content was found in green coffee beans (4.98%). In addition, instant coffee shows high CGA contents (4.75% and 4.21%, respectively). The most CA found was in instant coffee (1.61%) extracted with EtOH:water (3:2) and in spent coffee ground (1.11%) extracted with isopropanol:water (3:2). As expected, the CA values in green beans and the values of CGA and CA in cocoa shells were low.

It can be observed that the CGA content decreases from green beans to roasted beans, while the CA content increases. This is confirmed by literature where CA increases with increasing roasting times.[17–19]

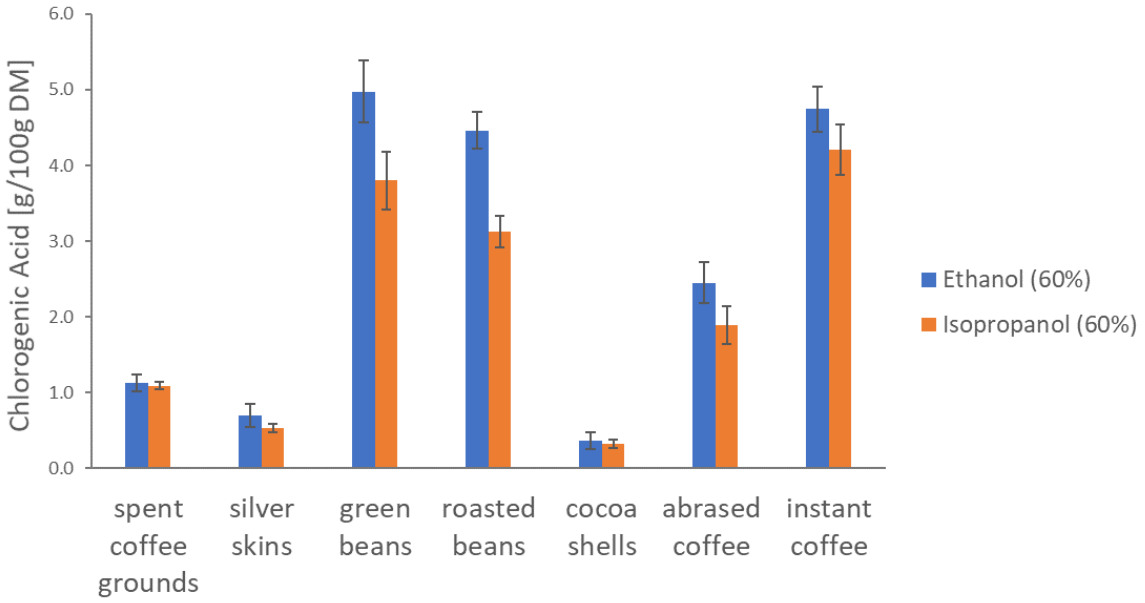

Figure 24: Yields of CGA extracted with EtOH:water (3:2) and Isopropanol:water (3:2), respectively. The values given are in g/100 g dry matter.

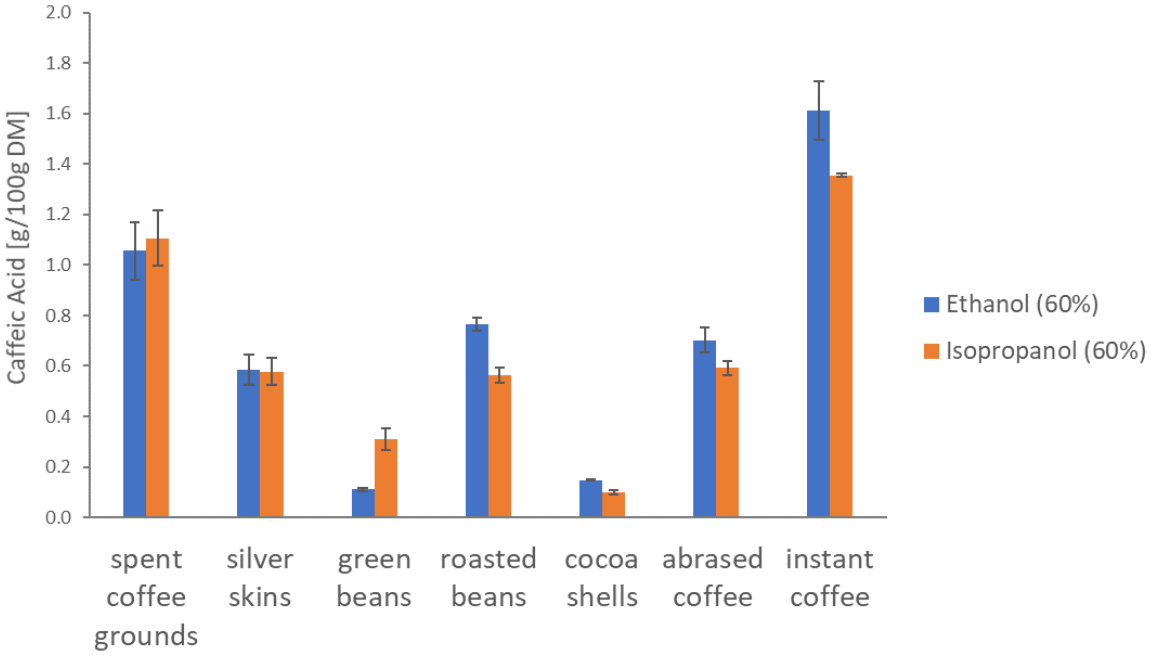

Figure 25: Yields of CA extracted with EtOH:water (3:2) and Isopropanol:water (3:2), respectively. The values given are in g/100 g dry matter.

4.2.5 Comparison of the TLC results with literature

For CGA and CA contents, different literature values with different extraction techniques and solvents used are summarised in **Table 5**-**6**. The major part of the available literature deals with CGA contents in green and roasted coffee beans, while sources for CA contents are limited.[14,26,53]

In general, the extractions were a success and the values determined in the frame of this thesis match with those in the literature. The only CGA used in the TLC analysis was 3-caffeoylquinic acid.[47] However, this should not be a problem as the other CGAs should have the same R_f values. It should also be pointed out that other substances can overlay at the same spot. The CGAs can be summed up as caffeoylquinic acids (3-, 4-, 5-CQA), di-caffeoylquinic acids (3,4-, 3,5-, 4,5-di-CQA) and feruloylquinic acid (4-, 5-FQA). Sometimes, also 3- and 5-coumaroylquinic acid and caffeoylquinic acid lactones are added to the total CGA value[54]. Unless otherwise stated, the total amount of CGA according to the corresponding literature is given. The literature values of green and roasted beans are Arabica (*Coffea Arabica*) and spent coffee grounds and coffee silver skins, which are presumably mixed (*Coffea Arabica* & *Coffea Canephora*). Differences in results can be explained by different coffee samples. The chemical composition depends on variety, growth region, climate, processing (harvesting time, purification, roasting, storage and packaging) and brewing.[18,22,55]

For spent coffee grounds, Bravo et al.[56] stated their result of 1.32 and 1.11 g/100 g as total CQAs + diCQAs, which matches with the experimentally obtained values of 1.13 and 1.09 g/100 g for EtOH (60%) and isopropanol (60%), respectively. Boyaszhieva et al.[57] (1.58 g/100 g) did not specify their CGA content at all.

In case of coffee silver skins, Bresciani et al.[54] summed up all the CGAs (0.59 g/100 g) named prior for their total CGA content. This matches with the obtained value of 0.70 and 0.54 g/100 g for EtOH (60%) and isopropanol (60%), respectively. Guglielmetti et al.[50] indicated their value of 0.27 g/100 g as 3-, 4-, 5-CQA, whereas Nzekoue et al.[53] only mentioned 3,5-diCQA, 3- and 5-CQA.

Table 5: Reported CGA content and comparison to the experimental values. AC means Activated carbon.

Source	Experimental [g/100 g DM] ± SD	Literature [g/100 g DM] ± SD	Solvent	Method	Ref.
spent coffee grounds	1.13 ± 0.11 (EtOH, 60%) 1.09 ± 0.05 (Iso.,60%)	1.32 ± n.d. 1.11 ± n.d.	H_2O	filter coffeemaker, 6 min, 90 °C	56
		1.40 ± 0.00	MeOH	Soxhlet extraction, 8 h	58
		1.58 ± 0.01	EtOH (48%)	vortex, 1 h, 70 °C	57
silver skins	0.70 ± 0.15 (EtOH, 60%) 0.54 ± 0.06 (Iso.,60%)	0.59 ± 0.07	H_2O	1% aq. formic acid, 30 min sonic bath; 70 °C, 1 h Dubnoff bath	54
		0.27 ± 0.00	EtOH (60%)	conventional solvent extraction, 30 min, 80°C	50
		0.54 ± 0.04 0.31 ± 0.01 0.46 ± 0.03 0.33 ± 0.01	MeOH H_2O MeOH EtOH (70%)	ultrasonic bath, 120 min, 20°C	53
green beans	4.98 ± 0.40 (EtOH, 60%) 3.80 ± 0.38 (Iso.,60%)	5.10 ± 0.47	H_2O	ultrasonic extraction, 1 min, boiled	14
		5.60 ± 0.14 4.95 ± 0.07 8.40 ± 0.28	MeOH EtOH H_2O	microwave assisted extraction, 5 min, 50 °C, 800 W	59
		5.07 ± 1.00 4.67 ± 1.60 5.28 ± 1.20	H_2O MeOH (70%) Isopropanol (60%)	80 °C, 30 min, stirring, AC 24 h, stirring, AC 48 h, stirring, AC	24
		6.67 ± 0.14	MeOH (70%)	overnight, stirring	23
		5.20 ± 0.07	MeOH (40%)	20 min, 300 rpm	21
roasted beans	4.46 ± 0.24 (EtOH, 60%) 3.13 ± 0.21 (Iso.,60%)	4.37 ± 0.11	MeOH (40%)	20 min, 300 rpm, light roast	21
		2.78 ± 0.21	MeOH (70%)	overnight, stirring	23
		1.30 ± 0.47	H_2O	ultrasonic extraction, boiled, 1 min	14
		4.46 ± 0.07	MeOH (70%)	soaked, 7h, RT	25
cocoa shells	0.37 ± 0.11 (EtOH, 60%) 0.33 ± 0.06 (Iso.,60%)	0.03 ± n.d.	H_2O	subcritical water extraction, 120 °C, 75 min, 20 mL/g	60

The general range of the CGA in green coffee beans (Arabica) investigated by Belitz et al.[22] is between 6.7 and 9.2%. This includes mono-, dicaffeoyl- and feruloylquinic acids. The main component is 5-CQA with a percentage of 3.0 - 5.6%. Suárez-Quiroz et al.[24] performed a purification with AC of 5-CQA from extracts with different solvents. AC was used as an adsorbent for the separation of phenols from food. Therefore, the aqueous extract was

adjusted to pH 3.0 with phosphoric acid. Then, 40 g/L AC was added and stirred for 30 minutes at 60 °C in the dark. The mixture was filtered, CGA was desorbed with ethanol 96% (v:v) and dried. Farah et al.[21] divided their total CGA content into the CQAs, FQAs and diCQAs. The green beans and light roasted coffee beans were chosen for the table. Here, the value of 5.20 g/100 g matches with the one of 4.98 g/100 g for EtOH (60%).

Only one source for cocoa shells could be found by Jokić et al.[60], which shows a lower result (0.03 g/100 g) than experimentally gained (0.37 and 0.33 g/100 g for EtOH (60%) and isopropanol (60%), respectively).

Table 6: Reported CA content and comparison to the experimental values.

Source	Experimental [g/100 g DM] ± SD	Literature [g/100 g DM] ± SD	Solvent	Method	Ref.
silver skins	0.59 ± 0.06 (EtOH, 60%) 0.58 ± 0.05 (Iso.,60%)	0.01 ± 0.00 0.01 ± 0.00 0.02 ± 0.00	H_2O MeOH EtOH (70%)	ultrasonic bath, 120 min, 20 °C	53
green beans	0.11 ± 0.01 (EtOH, 60%) 0.31 ± 0.04 (Iso.,60%)	0.27 ± n.d.	MeOH (70%)	ultrasonic extraction, 18 h, 4 °C	14
roasted beans	0.77 ± 0.03 (EtOH, 60%) 0.56 ± 0.03 (Iso.,60%)	0.18 ± n.d.	MeOH (70%)	ultrasonic extraction, 18 h, 4 °C	14
		1.2 ± n.d.	H_2O	extraction, 30 min.	26

Nzekoue et al.[53] achieved high values for CGA in coffee silver skins, but their CA content is low compared to the results determined in this thesis. Sunarharum[14] achieved similar results for the green, but not for the roasted beans compared to the experimental data. The exclusive (Coffee Arabica) mixed selection by Viesturs et al.[26] was chosen for literature comparison.

Conclusively, it can be stated that different types of coffee samples, growth region and especially the industrial processing steps give different results. Still, further research should be done in order to improve better comparability of coffee samples. One possible way would be the analysis of the same CGAs with the same analytical methods in different samples.

4.2.6 GC-MS analysis

In addition to the TLC analysis, GC-MS was carried out. Therefore, the samples were silanized for GC-MS measurements. Silylation reactions are most commonly used for derivatisation and substitute weakly bound hydrogen atoms from e.g. acids, alcohols and thiols by a trimethylsilyl group. Alternatives are alkylation and acylation. In alkylation reactions, the hydrogen atoms are substitute for an aliphatic or aliphatic-aromatic group. Acylation reagents transform hydrogen atom into esters, thioesters and amides which they cannot directly used for GC and need a purification step prior.[61] Li et al. (2009)[62] performed a GC-MS measurements using BSTFA-TMCS also as silylation reagent for CA and CGA identification in tobacco samples.

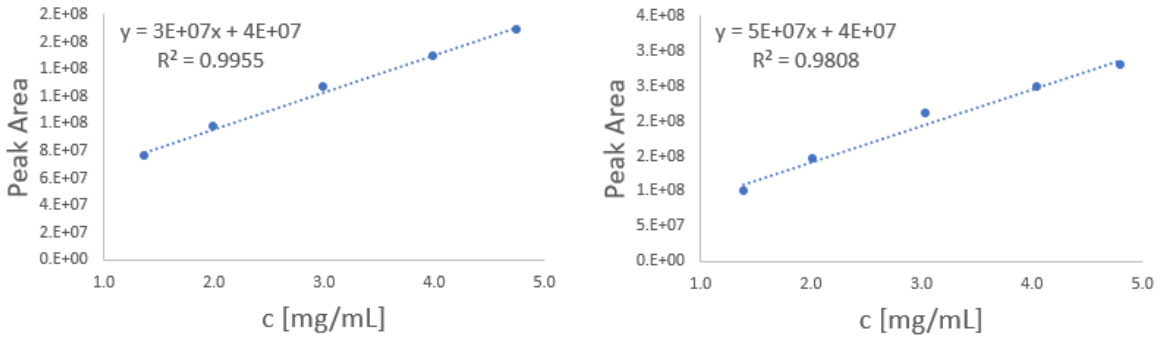

Figure 26: Calibration lines for GC-MS analysis of CGA (left) and CA (right).

For the content analysis, calibrations of CGA and CA were prepared and evaluated (**Figure 26**). For GC, CA has a retention time of 28.43 minutes and CGA has one of 56.11 minutes. The ion fragmentation scheme of 5-CQA is depicted in **Figure 27**.

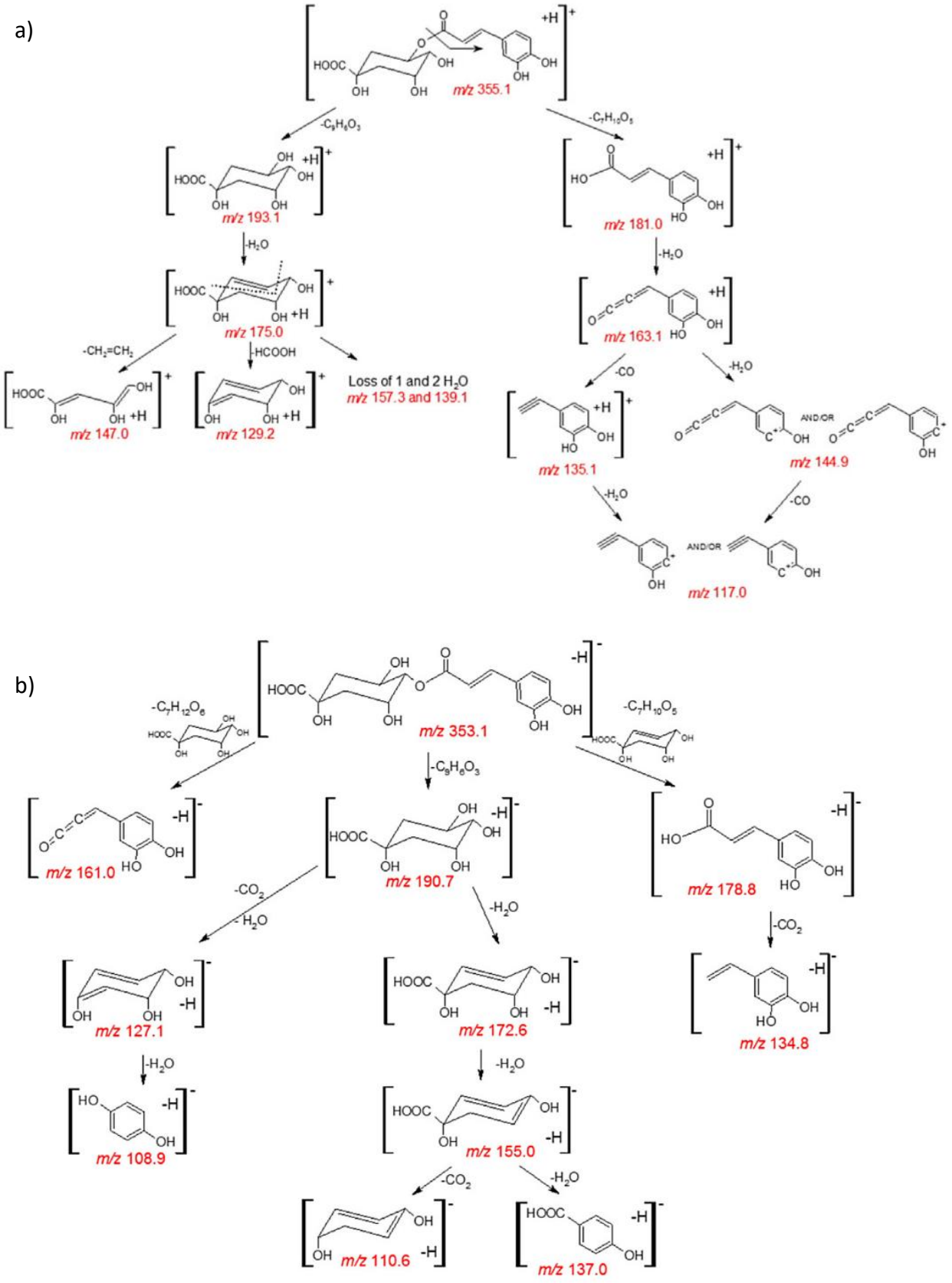

Figure 27: Positive (a) and negative (b) ion fragmentation of 5-CQA.[63]

The obtained results (**Table 7**) do not match with the TLC results or with any literature value (**Table 5-6**). The CGA and CA content in the extracts were outside the linear range of the calibration line and thus, this method could not be used for the evaluation.

Table 7: Results of the GC-MS measurements. Here, DM means dry matter and n.d. means not determined.

Source	EtOH:water (3:2) [g/100 g DM]		Isopropanol:water (3:2) [g/100 g DM]	
	CGA	CA	CGA	CA
spent coffee grounds	0.13	0.26	0.14	0.25
coffee silver skins	0.03	0.02	0.03	0.02
green beans	0.95	0.09	0.97	0.18
roasted beans	0.30	0.12	0.28	0.24
cocoa shells	n.d.	n.d.	n.d.	n.d.
abrased coffee	n.d.	0.12	n.d.	0.10
instant coffee	n.d.	0.28	n.d.	0.26

4.3 Solubility test of caffeic acid

In an RFB, the concentration of the electrolytes is very important, so a high solubility of the substrates is demanded. The higher the solubility of the redox couples, the better the energy density.[5]

Due to the problem with the noticeably low solubility of CA, a solubility test was carried out with adding a non-ionic surfactant (Tween®80) to see if it increases the solubility.[64] H_2O and 0.5 M H_3PO_4 were used as solvents. The measurement was carried out with a refractometer which determined the refractive index (RI). The RI value is dimensionless describing how fast light travels through a material. This value varies with different concentrations, resulting in a linear dependence. The corresponding calibrations are shown in **Figure 28**.

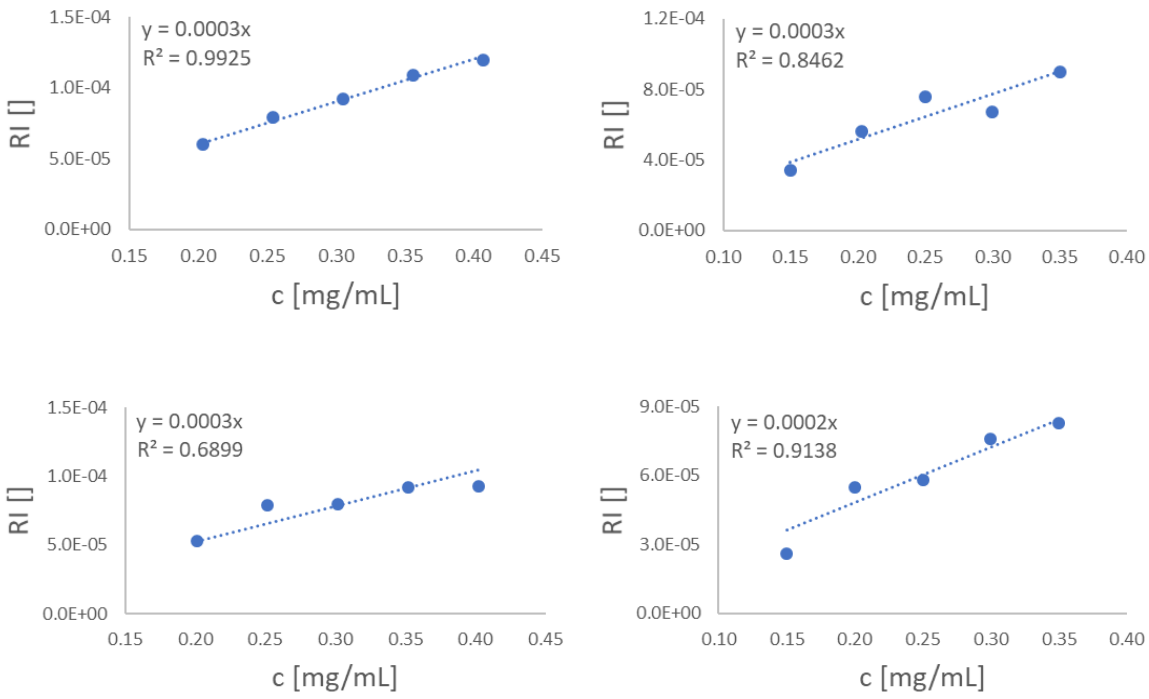

Figure 28: Calibrations of CA in H_2O (top left) and 0.5 M H_3PO_4 (bottom left), each with and without 0.5 w% Tween®80 (in H_2O: top right; in 0.5 M H_3PO_4: bottom right).

Table 8: Results of the solubility test of CA. n means amount of substance.

Solvent	Solubility [mg/mL]	n [mol/L]
dist. H_2O	0.686	0.004
dist. H_2O + 0.5 wt% Tween80	0.570	0.003
0.5 M H_3PO_4	1.066	0.006
0.5 M H_3PO_4 + 0.5 wt% Tween80	0.437	0.002

The results in **Table 8** show the low solubility of CA, mentioned before. There is a difference of 0.38 mg/mL between the solubility of H_2O and 0.5 M H_3PO_4. Also, the addition of Tween®80 (0.5 wt%) did not show any improvement. The solubility became worse by 16.9% for dist H_2O and by 59.0% for H_3PO_4 due to the surfactant might have formed micelles.

According to Mota et al.[65], the solubility of CA increased with the temperature of the solvent and decreasing pH-value. Using pure water at 23 °C a solubility of 0.98 g/L (pH = 3.37) was achieved in literature, which is much higher than the one obtained 0.686 mg/mL in dist. H_2O in the experiments of this work. Only the solubility of 1.066 mg/mL in 0.5 M H_3PO_4 tends to agree with the literature value of 0.98 g/L in pure water.[65,66]

4.4 Cyclic voltammetry (CV)

The purpose was to investigate whether pBQ, CA and CGA are suitable materials for RFBs. Therefore, the used solvents at various pH values were used for Pourbaix diagrams and the corresponding diffusion coefficients were calculated.

The substances were dissolved in H_3PO_4 and a citric acid phosphate buffer with different molarities and pH values, respectively. The pH values for the buffer system were 2.6, 2.8, 3.0, 3.2, 3.4, 4.0 and 4.5. The pH value for H_3PO_4 could be calculated as followed (**Equation 11**):

$$pH = 0.5 * (pK_a - \log(c_{HA})) \qquad \textbf{Equation 11}$$

In this equation the pK_a value of H_3PO_4 is 2.16 and the variable c_{HA} stands for the molarities of H_3PO_4, which are 0.01, 0.05, 0.1, 0.5 and 1 M. This results to pH values of 2.08, 1.73, 1.58, 1.23 and 1.08.

4.4.1 Pourbaix diagrams

The slopes of the Pourbaix diagrams indicate the nature of the electron transfer. A slope of -59 mV/pH unit indicates a two-electron transfer.[8] The slopes determined (**Figure 29-31**) indicate a single step two-electron two-proton transfer in acidic media. The corresponding cyclic voltammograms (CVs) are depicted in **Figure 32.**

Quinones (Q) undergo two one-electron reduction mechanism leading to a semiquinone ($Q^{\bullet -}$) and generating two cathodic reactions. The influence of a low pH increases the reaction rate, so that the hydroquinone (QH_2) can be formed directly as a product (**Scheme 1**).[67]

$$Q + e \rightleftharpoons Q^{\bullet -}$$
$$Q^{\bullet -} + H^+ \rightleftharpoons QH^{\bullet}$$
$$QH^{\bullet} + e \rightleftharpoons QH^-$$
$$QH^- + H^+ \rightleftharpoons QH_2$$

$$Q + 2H^+ + 2e \rightleftharpoons QH_2$$

Scheme 1: Reduction reaction of pBQ in aqueous media (left) and fast reaction mechanism (right).[67]

The slopes of -90.8 and -103.3 mV/pH for CGA in H_3PO_4 do not show fully reversibility. A reason might be that CGA could be adsorbed and thus be deposited on the electrode surface. In addition, all regressions show high accuracies except for pBQ and CA in H_3PO_4. The corresponding CVs can be found in **Figure 32**.

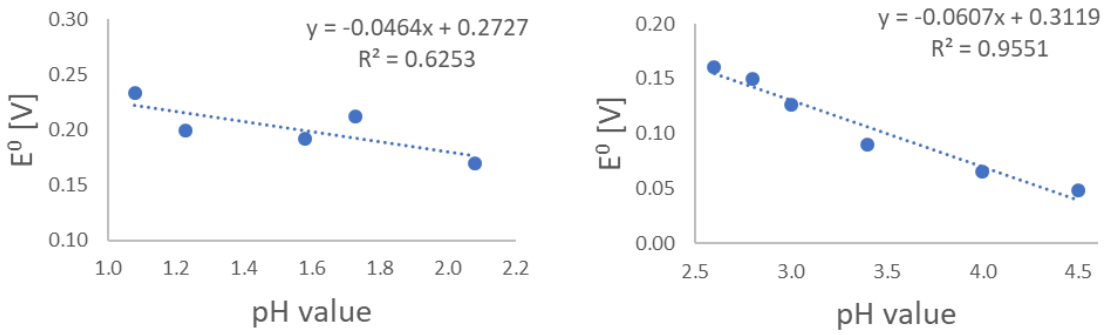

Figure 29: Pourbaix diagrams of pBQ in H_3PO_4 (left) and in buffer solution (right) at different pH values.

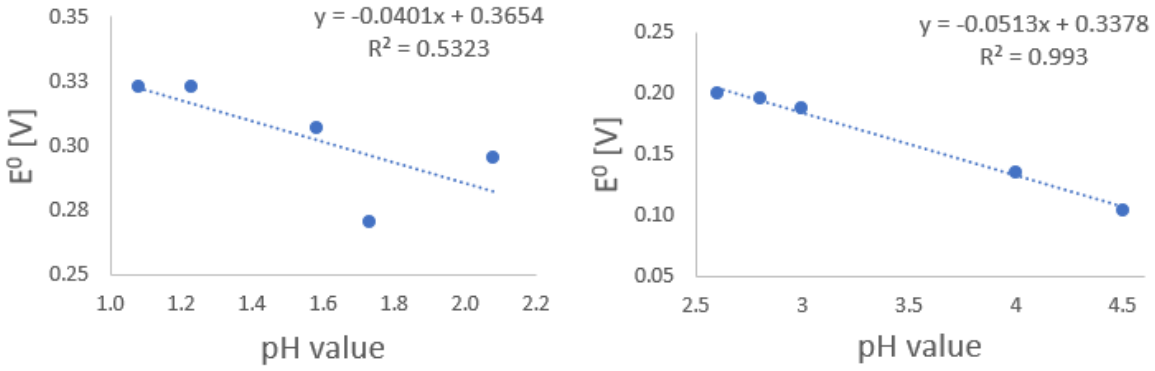

Figure 30: Pourbaix diagrams of CA in H_3PO_4 (left) and in buffer solution (right) at different pH values.

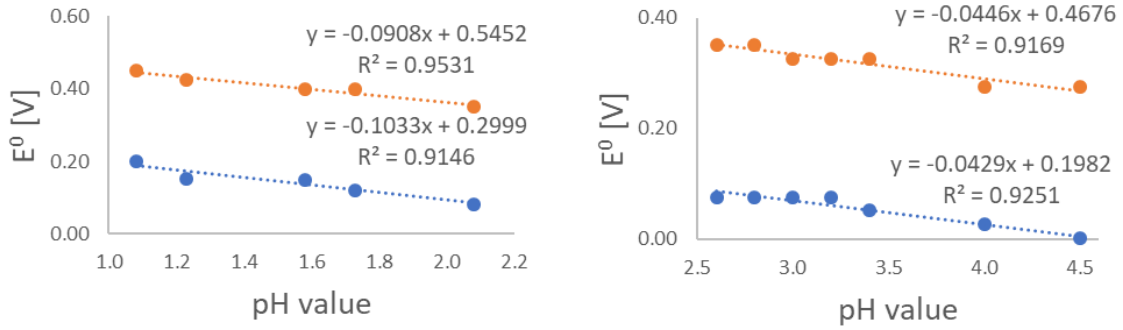

Figure 31: Pourbaix diagrams of CGA in H_3PO_4 (left) and in buffer solution (right) at different pH values.

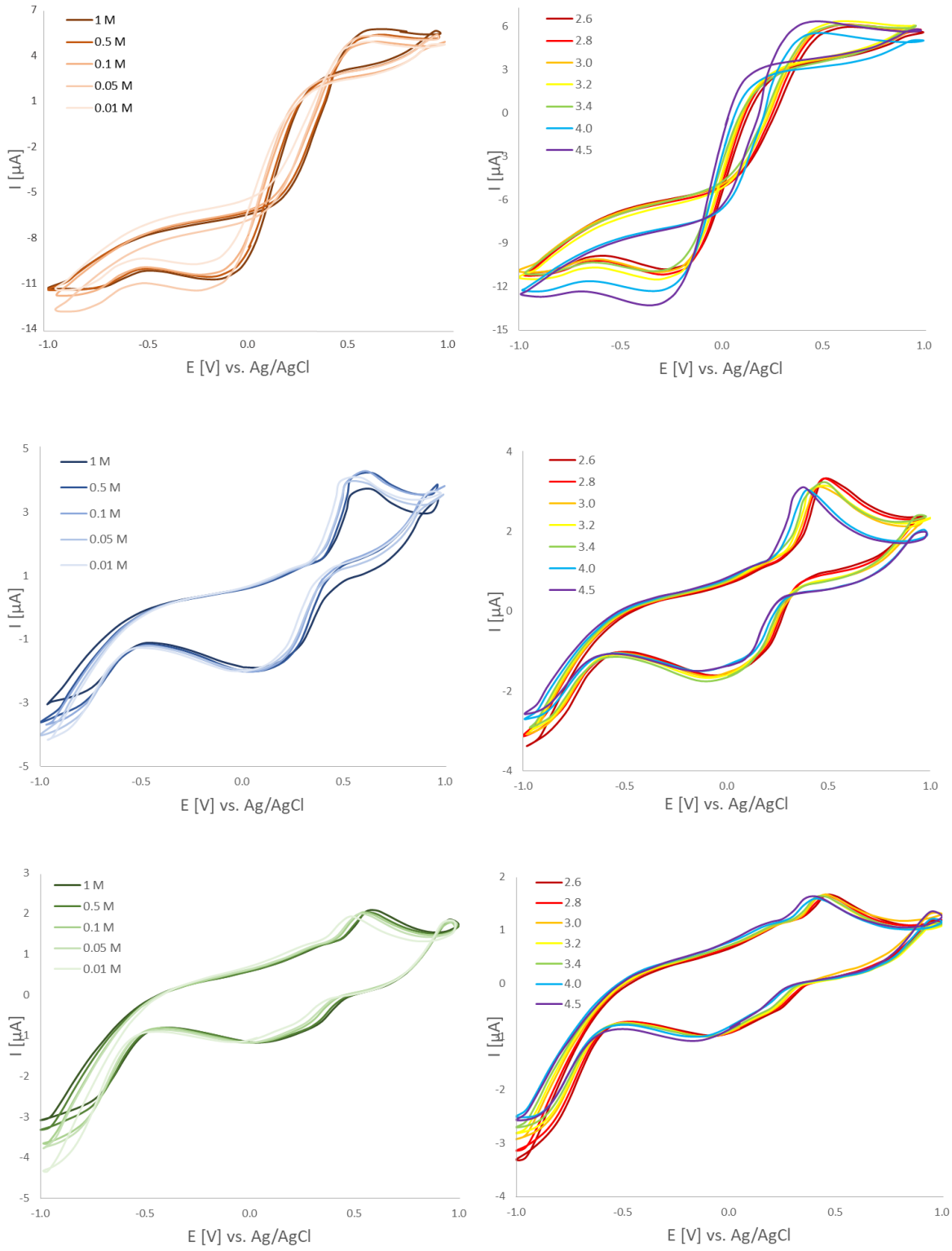

Figure 32: CVs of the Pourbaix diagrams for pBQ, CA and CGA (from top to bottom) in H_3PO_4 (left) and in buffer solution (right) at different pH values.

4.4.2 Stability test

The stability over 50 cycles was investigated by dissolving pBQ, CA and CGA in 0.5 M H_3PO_4 with a scan rate of 100 mV/s. The test indicates a stable system for all 50 cycles (**Figure 33**).

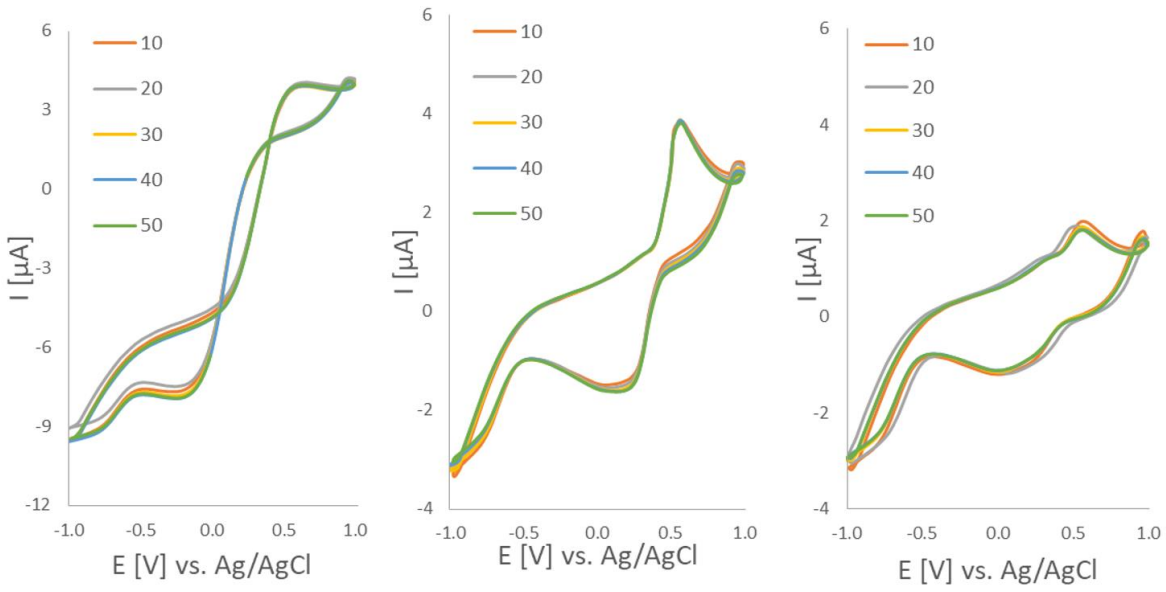

Figure 33: CVs of pBQ (0.51 mg), CA (0.57 mg) and CGA (0.98 mg) in 2 mL 0.5 M H_3PO_4 each with a scan rate of 100 mV/s. The cycles 10, 20, 30, 40 and 50 are shown.

4.4.3 Cyclic voltammograms of pBQ, CA and CGA

For the CVs the compounds (pBQ: 0.5 mg, CA: 0.5 mg, CGA: 1 mg) were dissolved in 0.5 M H_3PO_4 and in buffer solution with a pH value of 2.6. In general, **Figure 34** shows reversible redox processes for all substances. The voltammograms differ slightly depending on the solvent. For both CA and CGA, the peak currents are higher in H_3PO_4 than in buffer solution. The reason is that a buffer system remains its pH value when an acid is added in comparison to an unbuffered system. Thus, adding CA or CGA changes the pH in the 0.5 H_3PO_4 solution. However, pBQ lags at acid groups and therefore, the peak currents are similar.

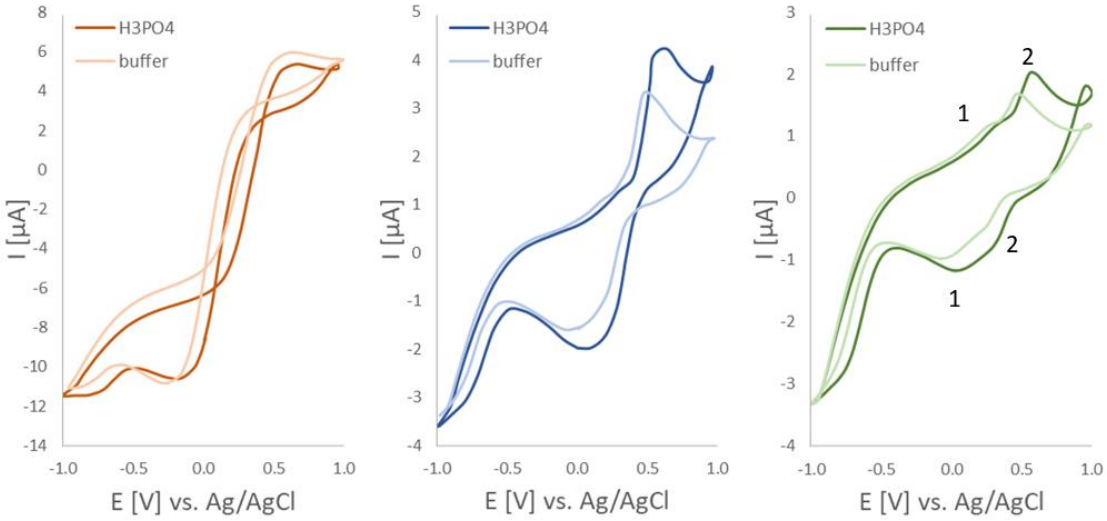

Figure 34: CVs of 0.52 and 0.49 mg pBQ (red), 0.53 and 0.51 mg CA (blue) and 1.06 and 1.06 mg CGA (green) in 2 mL 0.5 M H_3PO_4 (pH = 1.23) and buffer (pH = 2.6), respectively, with a scan rate of 100 mV/s.

CGA has two peaks, whereas the anodic peak 1 was difficult to evaluate. CGA (1 mg) achieves only half the peak current of CA (0.5 mg). The corresponding data to the CVs prior is shown in **Table 9**.

Table 9: Current maxima and redox potentials (E^0 vs. Ag/AgCl) of pBQ, CA and CGA with a scan rate of 100 mV/s.

0.5 M H_3PO_4	**I_{pa} [µA]**	**I_{pc} [µA]**	**E^0 [mV]**	
pBQ	5.36	-10.5	200	
CA	4.24	-1.98	323	
CGA	2.02	-0.78	153	peak 1
	1.15	-1.15	426	peak 2
buffer (pH = 2.6)				
pBQ	5.92	-10.83	160	
CA	3.33	-1.60	200	
CGA	1.15	-0.97	75	peak 1
	1.66	0.45	351	peak 2

The oxidation peak currents I_{pa} and reduction peak currents I_{pc} are not equivalent in all cases, except for the second peak of CGA in 0.5 M H_3PO_4. This proves a quasi-reversibility of the electrochemical behaviour of the compounds. The reduction mechanism is already depicted in **Scheme 1** and the oxidation mechanism of CA is shown in **Scheme 2**. The redox potentials E^0 of the ones in H_3PO_4 (0.5 M) are higher than in the buffer solution. The reason is the higher stability of quinones in highly acidic media. 0.5 M H_3PO_4 has a pH value of 1.23 whereas the buffer system has a higher one (pH = 2.6). This is the lowest possible pH value for this buffer system.

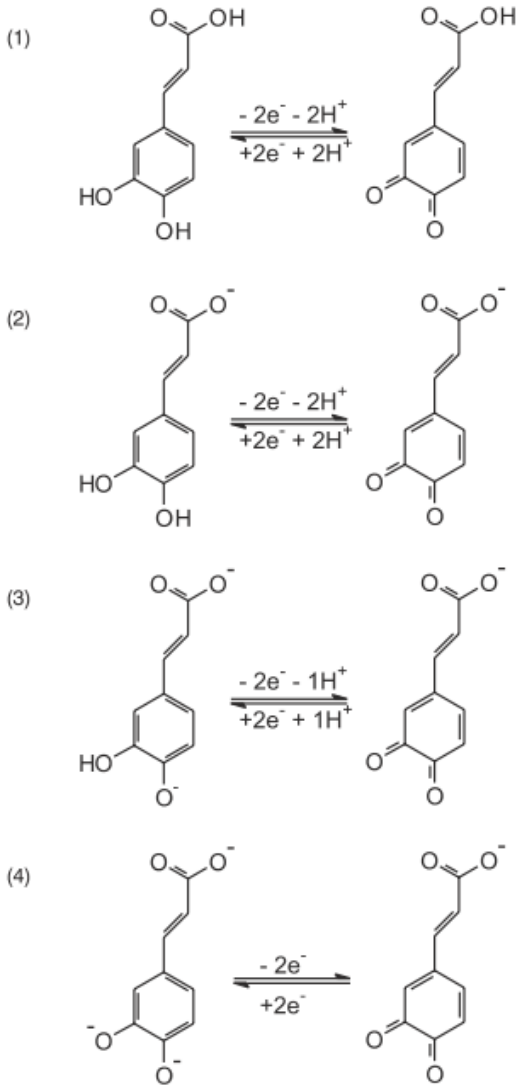

Scheme 2: Oxidation reactions for CA (H_3CAF (1), H_2CAF^-(2), $HCAF^{2-}$ (3), CAF^{3-} (4)).[68]

For the following discussion, the corresponding CVs and diagrams are depicted in **Figure 35-40** and the corresponding sample weights can be found in chapter 3.1.11 in **Table 1**.

For all investigated samples, the redox potentials (E^0) are independent of the scan rate (v). This indicates a stable E^0 and thus a stable system at various scan rates. **Figure 35-36** shows the CVs of pBQ in 0.5 M H_3PO_4 and buffer solution, respectively. In both voltammograms, the oxidation curves (anodic peak, E_{pa}) stay the same, whereas the reduction curves (cathodic peak, E_{pa}) shift with increasing scan rates. The plot of the current i_p against the square root of the scan rate $v^{1/2}$ of the oxidation and reduction peaks reflect this. The CVs of CA (**Figure 37-38**) show that both the anodic (i_{pa}) and cathodic peak (i_{pc}) maxima increase with increasing v. The same applies for CGA (**Figure 39-40**). Due to the linear dependency of the current i_p and the square root of the scan rate $v^{1/2}$, the used substances show a diffusion controlled behaviour.[27]

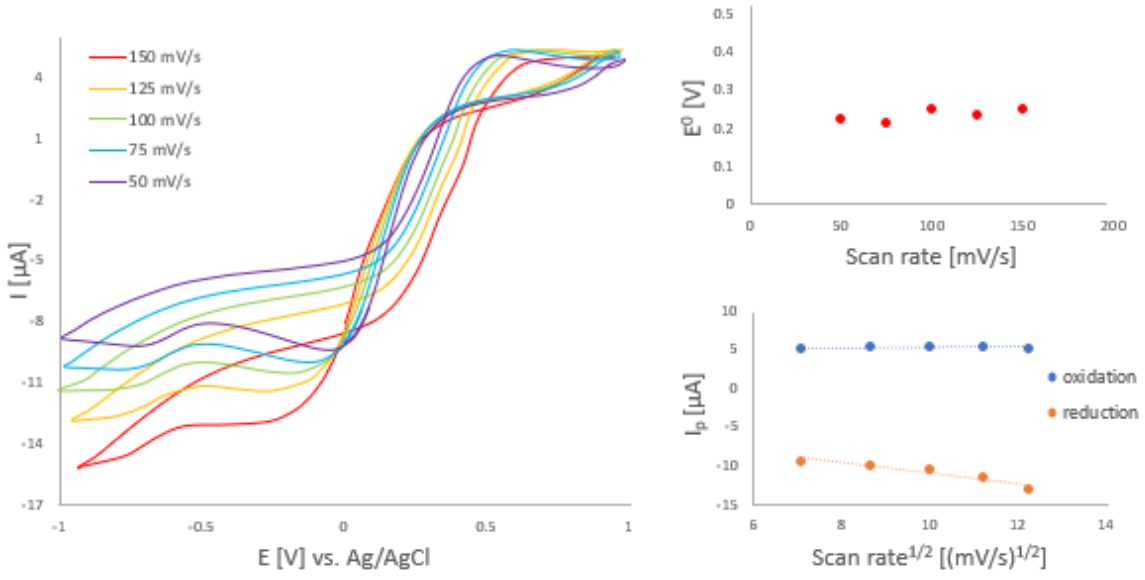

Figure 35: CVs of pBQ (0.52 mg) in 2 mL 0.5 M H_3PO_4 at various scan rates and the corresponding diagrams.

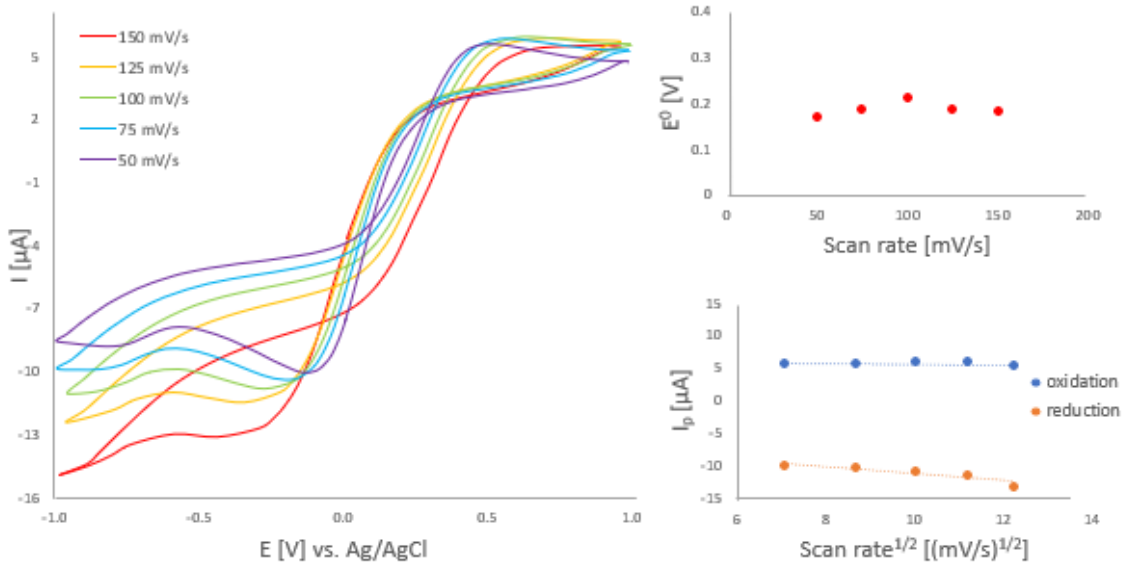

Figure 36: CVs of pBQ (0.49 mg) in 2 mL buffer solution (pH = 2.6) at various scan rates and the corresponding diagrams.

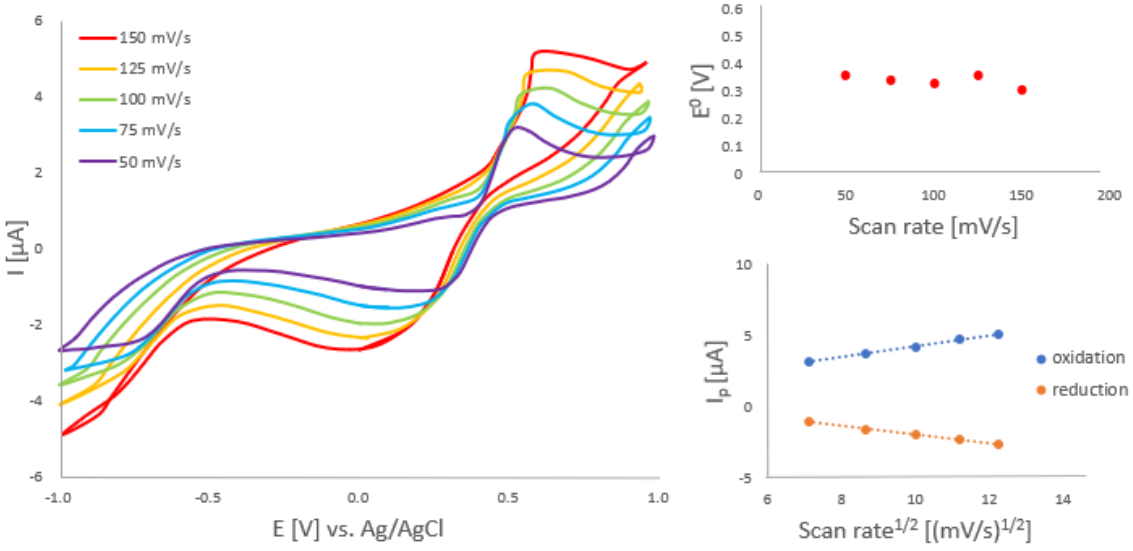

Figure 37: CVs of CA (0.53 mg) in 2 mL 0.5 M H_3PO_4 at various scan rates and the corresponding diagrams.

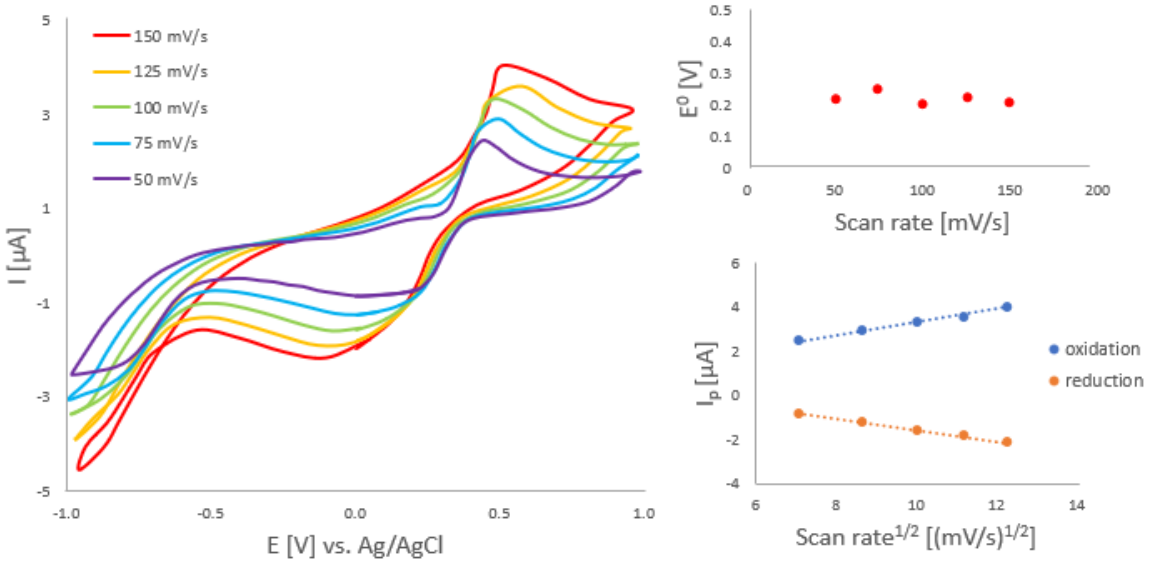

Figure 38: CVs of CA (0.51 mg) in 2 mL buffer solution (pH = 2.6) at various scan rates and the corresponding diagrams.

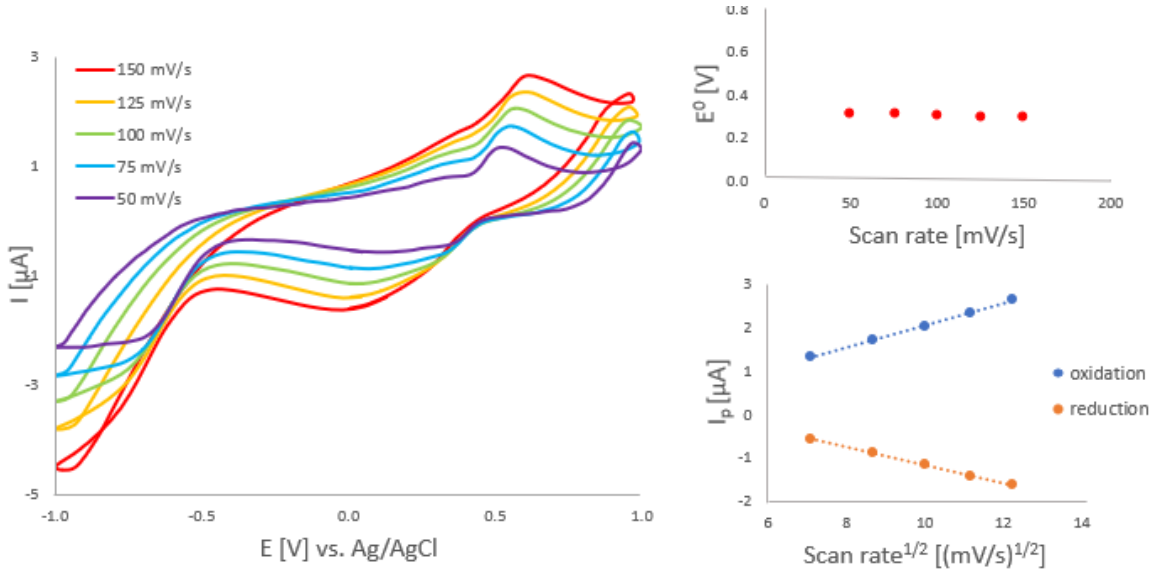

Figure 39: CVs of CGA (1.06 mg) in 2 mL 0.5 M H_3PO_4 at various scan rates and the corresponding diagrams.

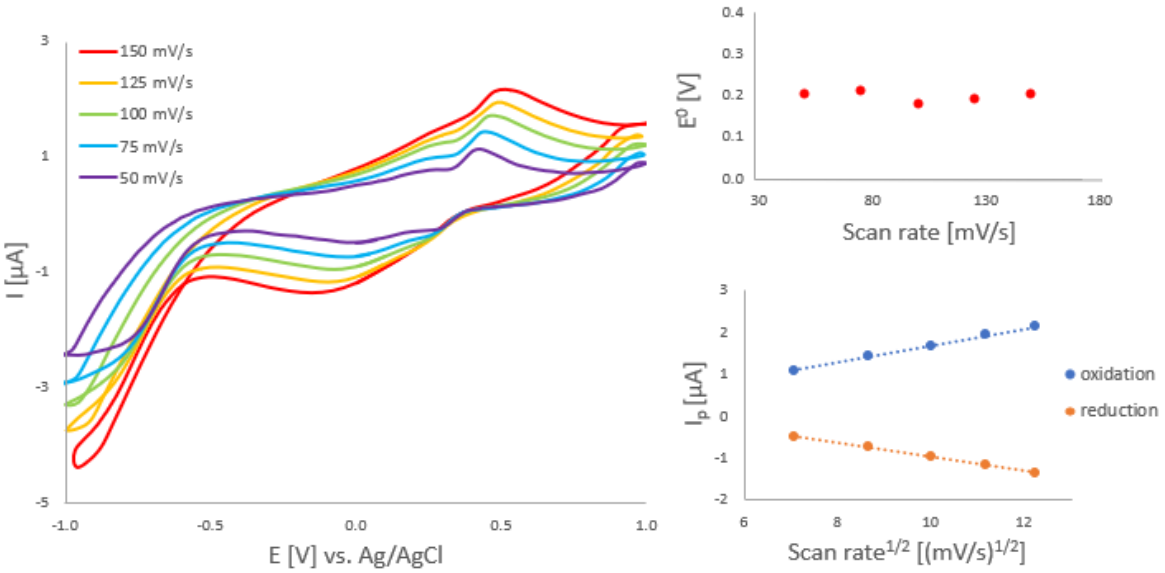

Figure 40: CVs of CGA (1.06 mg) in 2 mL buffer solution (pH = 2.6) at various scan rates and the corresponding diagrams.

4.4.4 Diffusion coefficient calculation

The diffusion coefficient was calculated according to the Randles-Sevcik equation[8] (**Equation 8**). The number of electrons transferred in a reversible system is two, which is typical for quinones[8].

The values are the average of the oxidation peaks at the different scan rates (**Table 10**). The calculated diffusion coefficients are similar between H_3PO_4 (0.5 M) and the buffer solution (pH = 2.6) of each source. However, pBQ and CA differ from CGA with a decimal power of one due to CGA having a higher molecular mass.

Namazian et al. (2005)[69] used a phosphate buffer for CGA with a diffusion coefficient of 1.46×10^{-8} cm^2/s. This is in the same order of magnitude as in this work. For CA no diffusion coefficient could be found for the used solvents.

Table 10: Comparison of calculated diffusion coefficient D in 0.5 M H_3PO_4 and in buffer solution (pH = 2.6) with literature.

Source	Calculated D [cm^2/s]	
	0.5 M H_3PO_4	buffer
pBQ	2.29×10^{-7}	3.19×10^{-7}
CA	3.68×10^{-7}	2.37×10^{-7}
CGA	7.73×10^{-8}	5.17×10^{-8}

4.4.5 Cyclic voltammograms of the extracts

The same measurements and evaluation were applied for the extracted samples as in the previous chapter (chapter 4.4.3). Therefore, 10 mL of extract solution were evaporated and the oily residues then were redissolved in 0.5 M H_3PO_4. In the case of instant coffee, only 4 mL were evaporated as there was too much residue at 10 mL.

The corresponding curves and diagrams can be found in **Figure 41-47**. All diagrams show that it has been proven that E^0 does not change with the scan rate. Also, the current increases with increasing scan rates.

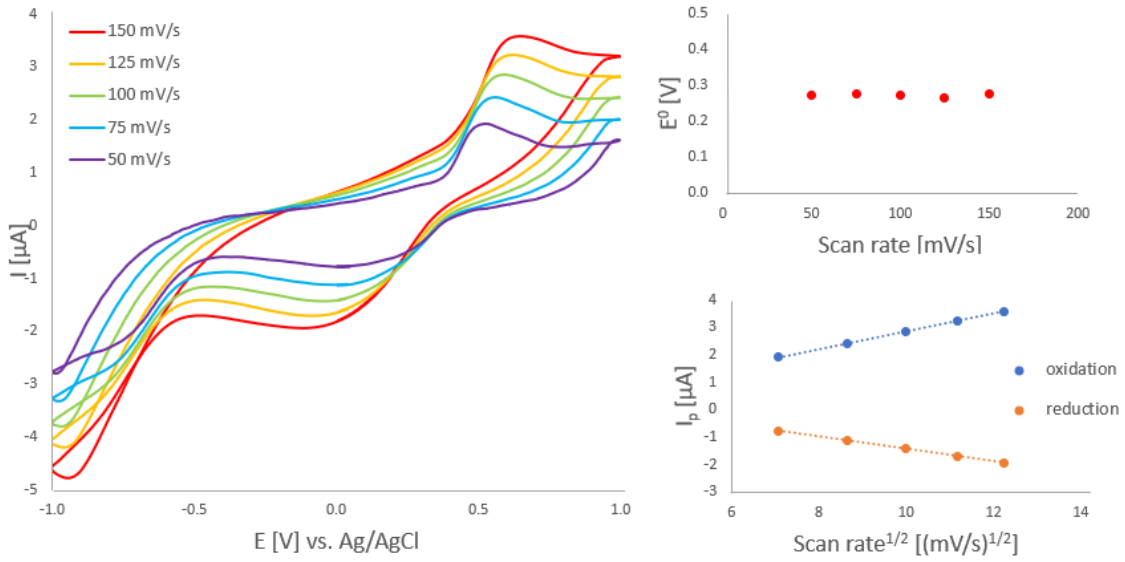

Figure 41: CVs of spent coffee grounds extract in 2 mL 0.5 M H_3PO_4 at various scan rates and the corresponding diagrams.

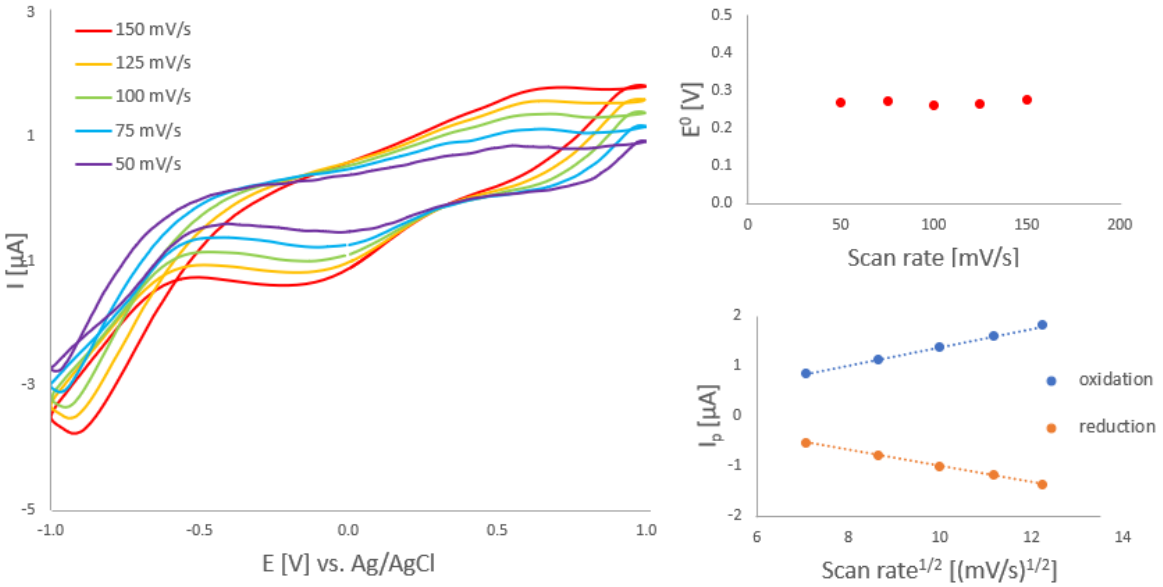

Figure 42: CVs of silver skins extract in 2 mL 0.5 M H_3PO_4 at various scan rates and the corresponding diagrams.

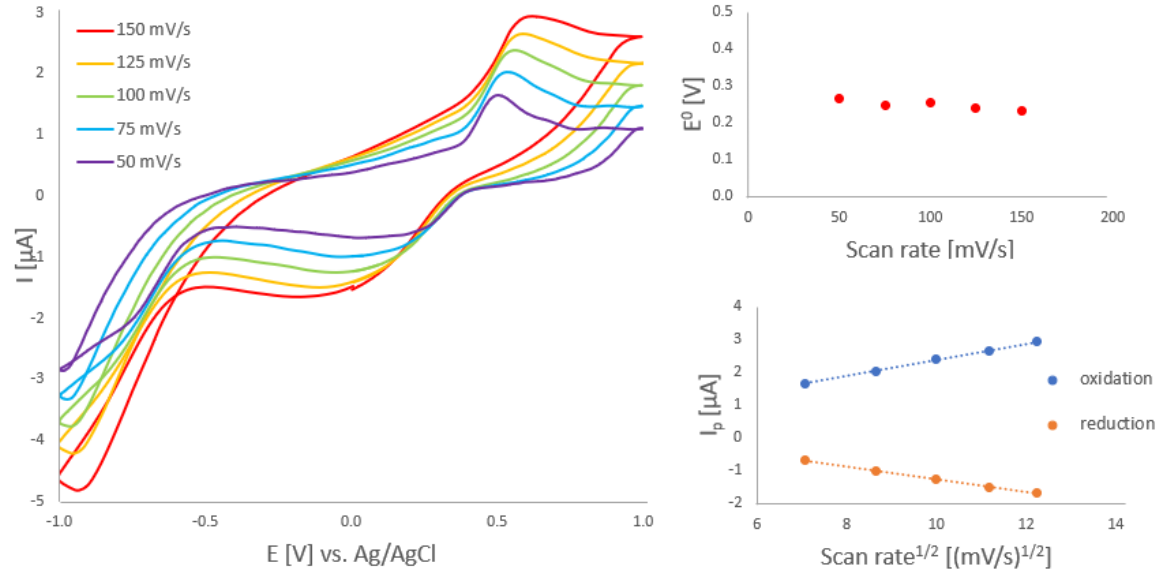

Figure 43: CVs of green coffee beans extract in 2 mL 0.5 M H_3PO_4 at various scan rates and the corresponding diagrams.

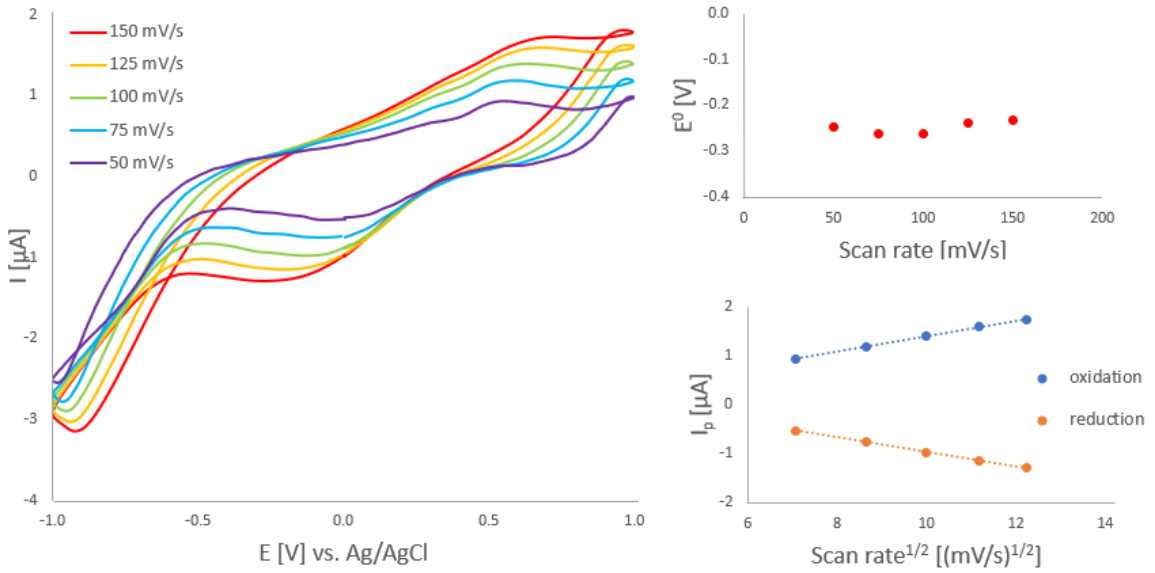

Figure 44: CVs of roasted coffee beans extract in 2 mL 0.5 M H_3PO_4 at various scan rates and the corresponding diagrams.

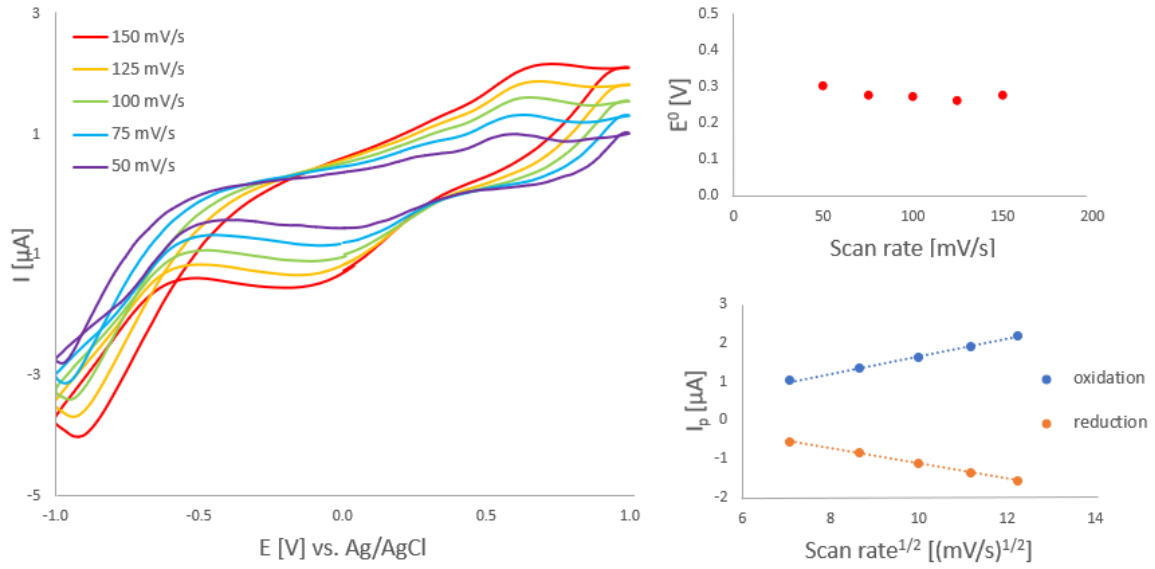

Figure 45: CVs of cocoa shells extract in 2 mL 0.5 M H_3PO_4 at various scan rates and the corresponding diagrams.

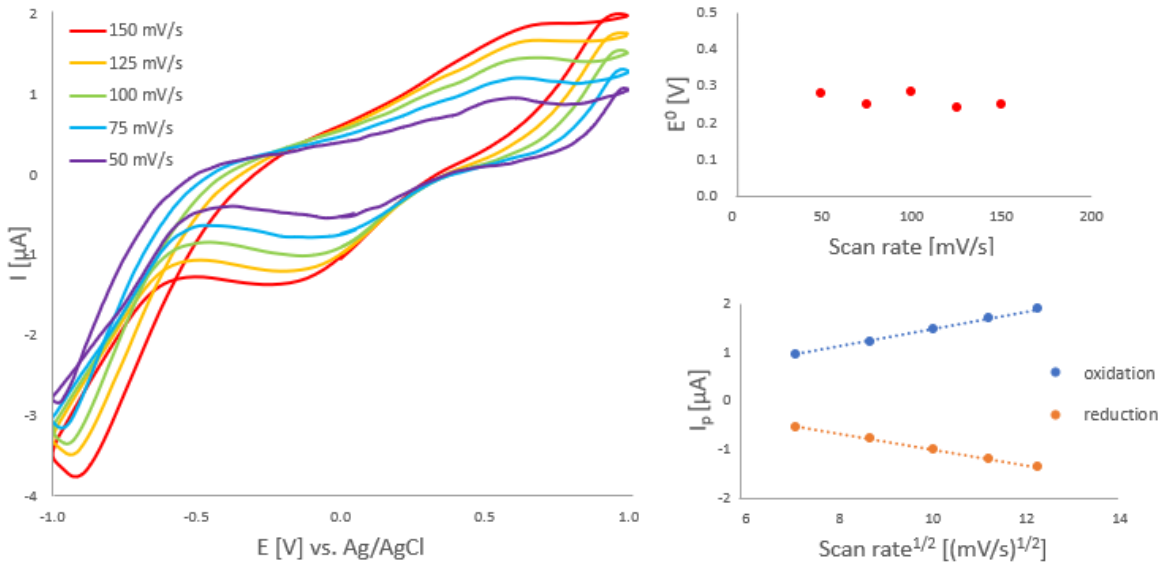

Figure 46: CVs of abrased coffee extract in 2 mL 0.5 M H_3PO_4 at various scan rates and the corresponding diagrams.

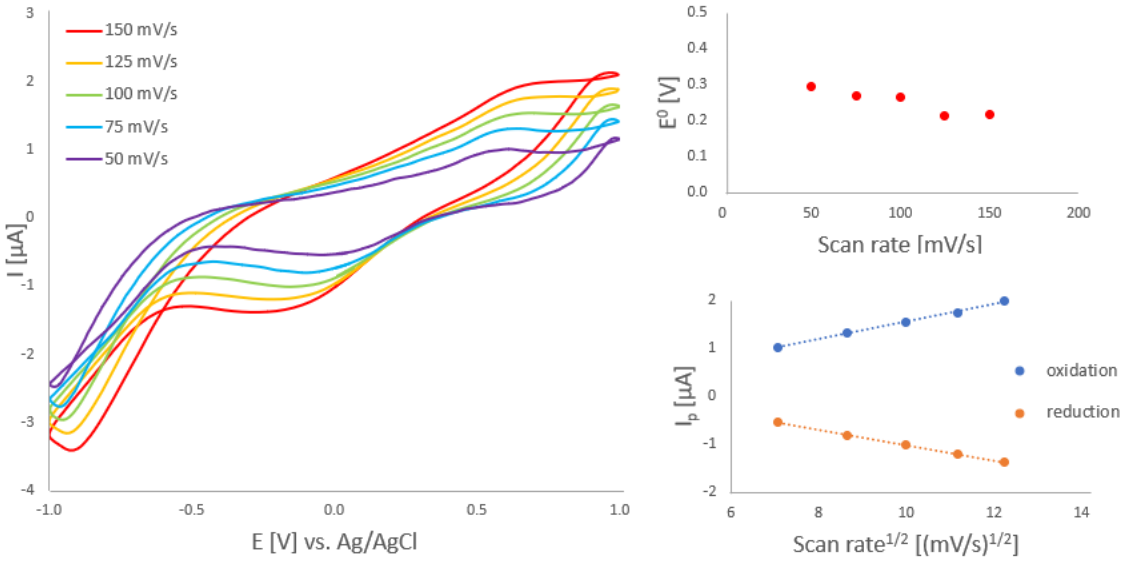

Figure 47: CVs of instant coffee extract in 2 mL 0.5 M H_3PO_4 at various scan rates and the corresponding diagrams.

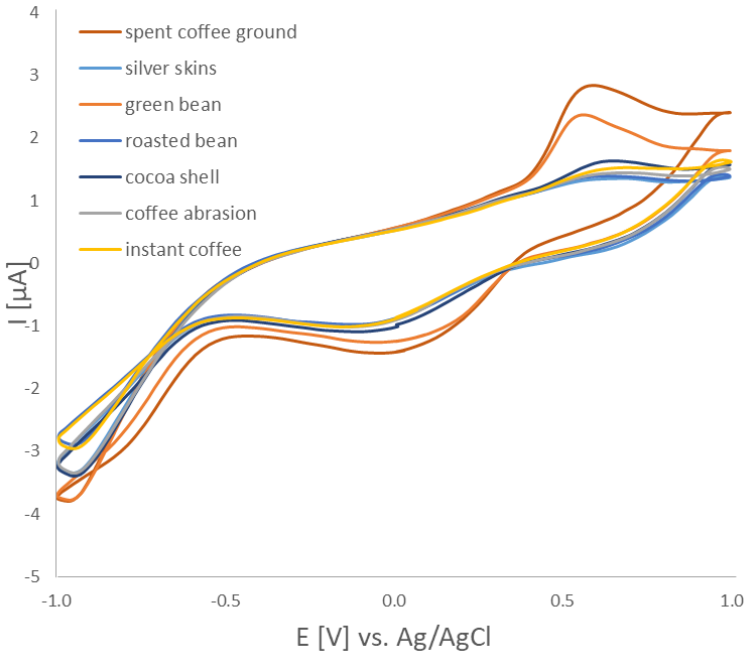

Figure 48: Comparison of the CVs of the sample extracts in 0.5 M H_3PO_4 with a scan rate of 100 mV/s.

The corresponding data of the CVs in **Figure 48** are shown in **Table 11**. The oxidation peak currents I_{pa} and reduction peak currents I_{pc} are not equivalent in all cases and show a quasi-reversibility for the pure substances. Spent coffee grounds and cocoa shells extracts have the same E^0 of 272 mV. Also, silver skins, roasted beans and instant coffee extracts have similar E^0 of 262, 262 and 263 mV, respectively. Abrased coffee has got the highest E^0 of 283 mV. Conclusively, the redox potentials are all in the same range.

However, the E^0 values are a bit lower than the ones of the pure substances in the same media. CA has an E^0 of 323 mV and CGA 153 and 426 mV. This could be due to other substances in the extracts.

Table 11: Weights, current maxima and redox potentials (E^0 vs. Ag/AgCl) of the extracts in H_3PO_4 (0.5 M) with a scan rate of 100 mV/s.

0.5 M H_3PO_4	Weight [mg]	I_{pa} [µA]	I_{pc} [µA]	E^0 [mV]
spent coffee grounds	28.7	2.85	-1.43	272
silver skins	33.7	1.36	1.00	262
green beans	53.7	2.38	-1.25	253
roasted beans	41.9	1.39	-0.98	262
cocoa shells	21.2	1.63	-1.09	272
abrased coffee	45.2	1.45	-1.01	283
instant coffee	51.4	1.54	-1.01	263

4.5 Redox flow cell

The theoretical capacity of the cell was calculated according to Faraday's first law of electrolysis[28] (**Equation 12**).

$$Q = n * z * F \qquad \textbf{Equation 12}$$

Q ... Total electric charge [C]
n .... Amount of substance [mole]
z..... Number of electrons transferred []
F .... Faraday constant [C/mol]

Two electrons are transferred in this cell, therefore, z = 2. The theoretical capacity was calculated using **Equation 13** and it was yielding 2.23 mAh.

$$Q_{th}\ [mAh] = \frac{2 * F * n}{3.6} \qquad \textbf{Equation 13}$$

The cell testing was carried out using 7.5 mg CA and 5 mg pBQ in slight excess as active materials in 35 mL of 0.5 M H_3PO_4 each. The flow rate was 150 mL/s, the charging/discharging time was 1.5 h at constant potentials of +0.75 V and -0.75 V, respectively. The results of the first 20 cycles are depicted in **Figure 49**.

Concerning the weight of CA used, the theoretical capacity was 298 mAh/g. The measured capacity only reached an average of 134 mAh/g (44.97%). This was 162 mAh/g lower than the theoretical capacity. The first five cycles achieved an average of at least 177 mAh/g (59.40%) which was 121 mAh/g lower than the theoretical value. Apart from this, the Coulomb efficiency was always close to 100%. Possible reasons for the poor performance could be the low solubility of CA, problems with the electrodes or the Nafion membrane. To eliminate problems, newly prepared electrodes and a new membrane were used resulting in the remaining issue of the poor solubility of CA.

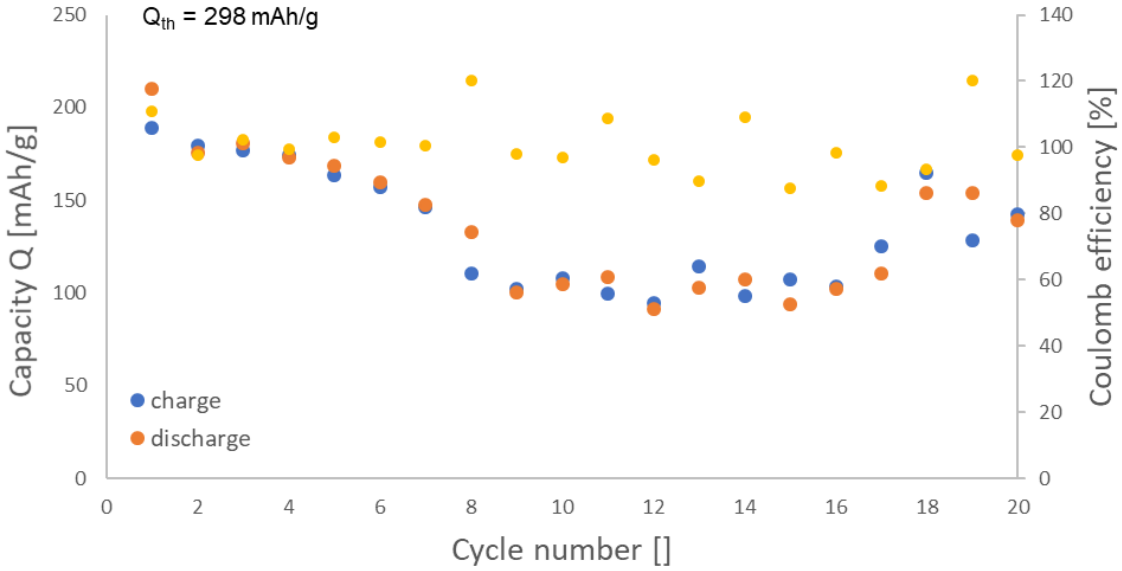

Figure 49: Potentiostatic cycling of the CA/pBQ redox flow cell. CA (7.5 mg) and pBQ (5 mg) as active materials were used in 0.5 M H_3PO_4 at ± 0.75 V with a charging/discharging time of 1.5 h. The flow rate was 150 mL/s.

5 Conclusion

The extraction of CGA and CA from the seven different samples was successfully carried out. The solvent mixtures (ethanol:water (3:2, v:v) and isopropanol:water (3:2, v:v), respectively) for the Soxhlet extraction are inexpensive and easy to handle. The best crude yield was achieved by the extraction with ethanol:water (3:2, v:v). However, there is still a need for optimisation as the high extraction times of 4.5 and 8.5 h are inconvenient. It might be possible to optimize the used extraction method regarding its duration, otherwise the method should be changed in favour of a more time saving one

The samples were successfully analysed with TLC. The GC-MS results could not be used, as the determined CGA and CA contents of the extracts are not located in the linear region of the calibration plot. In general, the TLC results fit well with the literature although it is difficult to compare as the spots are very likely to overlap and the literature values are from different coffee samples and CGAs.

The CV measurements proved that pBQ, CA and CGA are suitable materials for RFBs. Therefore, different molarities of H_3PO_4 and with different pH values of a 1 M citric acid and 2 M sodium phosphate dibasic dihydrate buffer system were used. The quinones (pBQ, CGA and CA) showed the expected linear dependency of the current i_p and the square root of the scan rate $v^{1/2}$. This proves the underlying redox reaction to be diffusion-controlled. Also, the quasi-reversibility was confirmed. All Pourbaix diagrams confirm the two-electron transfer of the quinones except for CGA in H_3PO_4. That indicates a not fully reversible system.

The poor redox flow cell experiments with CA and pBQ were not expected. The reason was probably the poor solubility of CA. However, slightly less than half the theoretical capacity of 298 mAh/g was achieved at an average of 100% constant coulomb efficiency. This indicates a basically functioning all-quinone RFB system with great potential for improvement in the future.

List of Abbreviations

AC..... Activated carbon

B..... 2-Butanone

BSTFA-TMCS ..... *N,O*-bis(trimethylsilyl)trifluoroacetamide

CA..... Caffeic acid

CGA ..... Chlorogenic acid

CGL..... Chlorogenic acid lactone

cmc..... Critical micelle concentration

CQA ..... Caffeoylquinic acid

CSS ..... Coffee silver skins

CV..... Cyclic Voltammetry

DM ..... Dry matter

EA..... Ethyl acetate

EtOH..... Ethanol

FA ..... Formic acid

GC-MS ..... Gas chromatography-Mass spectrometry

H_2O..... Water

H_2O_2 ..... Hydrogen peroxide

H_3PO_4 ..... Phosphoric acid

IEM..... Ion exchange membrane

KCl ..... Potassium chloride

KWh ..... Kilowatt hours

MWh ..... Megawatt hours

pBQ ..... *para*-Benzoquinone

PTFE ..... Polytetrafluoroethylene

RFB..... Redox Flow Battery

SCG..... Spent coffee grounds

SD..... Standard deviation

TLC ..... Thin Layer Chromatography

VRFB..... Vanadium Redox Flow Battery

List of Figures

List of Tables

List of Schemes

List of Equations

List of References

(1) Ellabban, O.; Abu-Rub, H.; Blaabjerg, F. Renewable energy resources: Current status, future prospects and their enabling technology. *Renew. Sust. Energ. Rev.* **2014**, *39*, 748–764.

(2) Koohi-Fayegh, S.; Rosen, M. A. A review of energy storage types, applications and recent developments. *J. Energy Storage.* **2020**, *27*, 101047.

(3) Shi, Y.; Eze, C.; Xiong, B.; He, W.; Zhang, H.; Lim, T. M.; Ukil, A.; Zhao, J. Recent development of membrane for vanadium redox flow battery applications: A review. *Appl. Energy.* **2019**, *238*, 202–224.

(4) Weber, A. Z.; Mench, M. M.; Meyers, J. P.; Ross, P. N.; Gostick, J. T.; Liu, Q. Redox flow batteries: a review. *J. Appl. Electrochem.* **2011**, *41*, 1137–1164.

(5) Wang, W.; Luo, Q.; Li, B.; Wei, X.; Li, L.; Yang, Z. Recent progress in redox flow battery research and development. *Adv. Funct. Mater.* **2013**, *23*, 970–986.

(6) Luo, Q.; Zhang, H.; Chen, J.; Qian, P.; Zhai, Y. Modification of Nafion membrane using interfacial polymerization for vanadium redox flow battery applications. *J. Membr. Sci.* **2008**, *311*, 98–103.

(7) https://www.vanadiumprice.com/ (17.03.2021).

(8) Wedege, K.; Dražević, E.; Konya, D.; Bentien, A. Organic redox species in aqueous flow batteries: Redox potentials, chemical stability and solubility. *Sci. Rep.* **2016**, *6*, 39101.

(9) Singh, V.; Kim, S.; Kang, J.; Byon, H. R. Aqueous organic redox flow batteries. *Nano Res.* **2019**, *12*, 1988–2001.

(10) Leung, P.; Shah, A. A.; Sanz, L.; Flox, C.; Morante, J. R.; Xu, Q.; Mohamed, M. R.; Ponce de León, C.; Walsh, F. C. Recent developments in organic redox flow batteries: A critical review. *J. Power Sources* **2017**, *360*, 243–283.

(11) Yang, B.; Hoober-Burkhardt, L.; Wang, F.; Prakash, G. K. S.; Narayanan, S. R. An inexpensive aqueous flow battery for large-scale electrical energy storage based on water-soluble organic redox couples. *J. Electrochem. Soc.* **2014**, *161*, A1371-A1380.

(12) Schlemmer, W.; Nothdurft, P.; Petzold, A.; Frühwirt, P.; Schmallegger, M.; Gescheidt-Demner, G.; Fischer, R.; Freunberger, S. A.; Kern, W.; Spirk, S.

2-Methoxyhydroquinone from vanillin for aqueous redox-flow batteries. *Angew. Chem. Int. Ed.* **2020**, 22943–22946.

(13) Naveed, M.; Hejazi, V.; Abbas, M.; Kamboh, A. A.; Khan, G. J.; Shumzaid, M.; Ahmad, F.; Babazadeh, D.; FangFang, X.; Modarresi-Ghazani, F.*; et al.* Chlorogenic acid (CGA): A pharmacological review and call for further research. *Biomed. Pharmacother.* **2018**, *97*, 67–74.

(14) Sunarharum, W. B. The compositional basis of coffee flavour. Dissertation, The University of Queensland, Brisbane, Australia, **2016**.

(15) Pedras, B. M.; Nascimento, M.; Sá-Nogueira, I.; Simões, P.; Paiva, A.; Barreiros, S. Semi-continuous extraction/hydrolysis of spent coffee grounds with subcritical water. *J. Ind. Eng. Chem.* **2019**, *72*, 453–456.

(16) Mills, C. E.; Oruna-Concha, M. J.; Mottram, D. S.; Gibson, G. R.; Spencer, J. P. E. The effect of processing on chlorogenic acid content of commercially available coffee. *Food Chem.* **2013**, *141*, 3335–3340.

(17) Matta, F. V. Mini-Review of the chemical composition of toasting brazillian coffee. *Act. Sci. Nutr. Health.* **2019**, *3*, 2582-1423.

(18) del Castillo, M. D.; Ames, J. M.; Gordon, M. H. Effect of roasting on the antioxidant activity of coffee brews. *J. Agric. Food Chem.* **2002**, *50*, 3698–3703.

(19) Diviš, P.; Pořízka, J.; Kříkala, J. The effect of coffee beans roasting on its chemical composition. *Potr. S. J. F. Sci.* **2019**, *13*, 344–350.

(20) Bauer, D.; Abreu, J.; Jordão, N.; Rosa, J. S. d.; Freitas-Silva, O.; Teodoro, A. Effect of roasting levels and drying process of coffea canephora on the quality of bioactive compounds and Cytotoxicity. *Int. J. Mol. Sci.* **2018**, *19*.

(21) Farah, A.; Paulis, T. de; Trugo, L. C.; Martin, P. R. Effect of roasting on the formation of chlorogenic acid lactones in coffee. *J. Agr. Food. Chem.* **2005**, *53*, 1505–1513.

(22) Belitz, H.-D., Grosch, W., & Schieberle, P. *Food chemistry*; Springer Berlin Heidelberg: Berlin, Heidelberg, **2009**.

(23) Moreira, A. S. P.; Nunes, F. M.; Simões, C.; Maciel, E.; Domingues, P.; Domingues, M. R. M.; Coimbra, M. A. Transglycosylation reactions, a main mechanism of phenolics

incorporation in coffee melanoidins: Inhibition by Maillard reaction. *Food Chem.* **2017**, *227*, 422–431.

(24) Suárez-Quiroz, M. L.; Alonso Campos, A.; Valerio Alfaro, G.; González-Ríos, O.; Villeneuve, P.; Figueroa-Espinoza, M. C. Isolation of green coffee chlorogenic acids using activated carbon. *J. Food Compos. Anal.* **2014**, *33*, 55–58.

(25) Moon, J.-K.; Yoo, H. S.; Shibamoto, T. Role of roasting conditions in the level of chlorogenic acid content in coffee beans: correlation with coffee acidity. *J. Agr. Food Chem.* **2009**, *57*, 5365–5369.

(26) Viesturs Kreicbergs; Fredijs Dimins; Velga Mikelsone; Ingmars Cinkmanis. Biologically active compounds in roasted coffee. FoodBalt-2011. 6th Baltic Conference on Food Science and Technology. **2011**, 110–115.

(27) Elgrishi, N.; Rountree, K. J.; McCarthy, B. D.; Rountree, E. S.; Eisenhart, T. T.; Dempsey, J. L. A practical beginner's guide to cyclic voltammetry. *J. Chem. Educ.* **2018**, *95*, 197–206.

(28) Bard, A. J.; Faulkner, L. R. Electrochemical methods: Fundamentals and applications, 2nd ed.; Wiley: New York, **2001**.

(29) Pourbaix, M. Atlas of electrochemical equilibria in aqueous solutions. Pergamon Press Ltd., USA. **1966**.

(30) Batchelor-McAuley, C.; Li, Q.; Dapin, S. M.; Compton, R. G. Voltammetric characterization of DNA intercalators across the full pH range: anthraquinone-2,6-disulfonate and anthraquinone-2-sulfonate. *J. Phys. Chem. B.* **2010**, *114*, 4094–4100.

(31) http://www.fao.org/3/a-i4985e.pdf (Food and Agriculture Organization of the United Nations, Statistical Pocketbook Coffee, 2015) (13.01.2021).

(32) https://www.kaffee-frei-haus.com/en_IE/coffee/cultivation/growing-areas/ (26.01.2021).

(33) ICO, 2020. Coffee production, www.ico.org. (13.01.2021).

(34) Narita, Y.; Inouye, K. Review on utilization and composition of coffee silverskin. *Food Res. Int.* **2014**, *61*, 16–22.

(35) Janissen, B.; Huynh, T. Chemical composition and value-adding applications of coffee industry by-products: A review. *Resour. Conserv. Recycl.* **2018**, *128*, 110–117.

(36) Murthy, P. S.; Madhava Naidu, M. Sustainable management of coffee industry by-products and value addition—A review. *Resour. Conserv. Recycl.* **2012**, *66*, 45–58.

(37) Karmee, S. K. A spent coffee grounds based biorefinery for the production of biofuels, biopolymers, antioxidants and biocomposites. *Waste Manage.* **2018**, *72*, 240–254.

(38) Dean, J. R. *Extraction methods for environmental analysis.*; John Wiley: Chichester, New York, **1998**.

(39) Castro, L.M.D. de; Ayuso, L. E. Soxhlet extraction. **2000**, 2701-2709.

(40) https://imagej.net/Fiji/Downloads (12.10.2020).

(41) http://www.ico.org/documents/iccres420e.pdf (26.10.2020).

(42) Caballero, B.; Trugo, L. C.; Finglas, P.; Toldra, F. Encyclopedia of food sciences and nutrition. **2003**, 1498–1506.

(43) François L. Guillot, Armand Malnoë, and Richard H. Stadler. Antioxidant properties of novel tetraoxygenated phenylindan isomers formed during thermal decomposition of caffeic acid. *J. Agric. Food. Chem.* **1996**, 2503–2510.

(44) López-Barrera, D. M.; Vázquez-Sánchez, K.; Loarca-Piña, M. G. F.; Campos-Vega, R. Spent coffee grounds, an innovative source of colonic fermentable compounds, inhibit inflammatory mediators in vitro. *Food Chem.* **2016**, *212*, 282–290.

(45) Borrelli, R. C.; Esposito, F.; Napolitano, A.; Ritieni, A.; Fogliano, V. Characterization of a new potential functional ingredient: coffee silverskin. *J. Agr. Food Chem.* **2004**, *52*, 1338–1343.

(46) Osundahunsi, O. F.; Bolade, M. K.; Akinbinu, A. A. Effect of cocoa shell ash as an alkalizing agent on cocoa products. *J. Appl. Sci.* **2007**, *7*, 1674–1678.

(47) https://www.fishersci.com/shop/products/chlorogenic-acid-predominantly-trans-from-coffee-seeds-99-acros-organics-2/AC109240010 (24.04.2020).

(48) https://www.alfa.com/de/catalog/A15950/ (24.04.2020).

(49) Ji, W.; Meng, Q.; Ding, L.; Wang, F.; Dong, J.; Zhou, G.; Wang, B. Measurement and correlation of the solubility of caffeic acid in eight mono and water+ethanol mixed solvents at temperatures from (293.15 to 333.15) K. *J. Mol. Liq.* **2016**, *224*, 1275–1281.

(50) Guglielmetti, A.; D'Ignoti, V.; Ghirardello, D.; Belviso, S.; Zeppa, G. Optimisation of Ultrasound and Mirowave-Assisted Extraction of Caffeoylquinic Acids and Caffeine

from Silverskin using Response Surface Methodology. *Ital. J. Food Sci.* **2017**, 409–423.

(51) Vrije, T. de; Budde, M.; van der Wal, H.; Claassen, P. A. M.; López-Contreras, A. M. "In situ" removal of isopropanol, butanol and ethanol from fermentation broth by gas stripping. *Bioresour. Technol.* **2013**, *137*, 153–159.

(52) Kanokwan, K.; Thananya, N.; Pimporn, L. Evaluation of antioxidant and anti-tyrosinase activities as well as stability of green and roasted coffee bean extracts from Coffea arabica and Coffea canephora grown in Thailand. *J. Pharmacognosy Phytother.* **2016**, *8*, 182–192.

(53) Nzekoue, F. K.; Angeloni, S.; Navarini, L.; Angeloni, C.; Freschi, M.; Hrelia, S.; Vitali, L. A.; Sagratini, G.; Vittori, S.; Caprioli, G. Coffee silverskin extracts: Quantification of 30 bioactive compounds by a new HPLC-MS/MS method and evaluation of their antioxidant and antibacterial activities. *Food Res. Int.* **2020**, *133*, 109128.

(54) Bresciani, L.; Calani, L.; Bruni, R.; Brighenti, F.; Del Rio, D. Phenolic composition, caffeine content and antioxidant capacity of coffee silverskin. *Food Res. Int.* **2014**, *61*, 196–201.

(55) Matei, M. F.; Jaiswal, R.; Kuhnert, N. Investigating the chemical changes of chlorogenic acids during coffee brewing: conjugate addition of water to the olefinic moiety of chlorogenic acids and their quinides. *J. Agric. Food. Chem.* **2012**, *60*, 12105–12115.

(56) Bravo, J.; Juániz, I.; Monente, C.; Caemmerer, B.; Kroh, L. W.; Peña, M. P. de; Cid, C. Evaluation of spent coffee obtained from the most common coffeemakers as a source of hydrophilic bioactive compounds. *J. Agr. Food. Chem.* **2012**, *60*, 12565–12573.

(57) Boyadzhieva, S.; Angelov, G.; Georgieva, S.; Yankov, D. Characterization of polyphenol content and antioxidant capacity of spent coffee grounds. *Bulg. Chem. Commun.* **2018**, 85–89.

(58) Ramalakshmi, K.; Rao, L. J. M.; Takano-Ishikawa, Y.; Goto, M. Bioactivities of low-grade green coffee and spent coffee in different in vitro model systems. *Food Chem.* **2009**, *115*, 79–85.

(59) Upadhyay, R.; Ramalakshmi, K.; Jagan Mohan Rao, L. Microwave-assisted extraction of chlorogenic acids from green coffee beans. *Food Chem.* **2012**, *130*, 184–188.

(60) Jokić, S.; Gagić, T.; Knez, Ž.; Šubarić, D.; Škerget, M. Separation of active compounds from food by-product (cocoa shell) using subcritical water Extraction. *Molecules* **2018**, *23*.

(61) Schummer, C.; Delhomme, O.; Appenzeller, B. M. R.; Wennig, R.; Millet, M. Comparison of MTBSTFA and BSTFA in derivatization reactions of polar compounds prior to GC/MS analysis. *Talanta.* **2009**, *77*, 1473–1482.

(62) Li, F.; Liu, Q.; Cai, W.; Shao, X. Analysis of scopoletin and caffeic acid in tobacco by GC–MS After a rapid derivatization procedure. *Chroma.* **2009**, *69*, 743–748.

(63) Willems, J. L.; Khamis, M. M.; Mohammed Saeid, W.; Purves, R. W.; Katselis, G.; Low, N. H.; El-Aneed, A. Analysis of a series of chlorogenic acid isomers using differential ion mobility and tandem mass. spectrometry. *Anal. Chim. Acta.* **2016**, *933*, 164–174.

(64) Stoyanova, K.; Vinarov, Z.; Tcholakova, S. Improving Ibuprofen solubility by surfactant-facilitated self-assembly into mixed micelles. *J. Drug Deliv. Sci. Technol.* **2016**, *36*, 208–215.

(65) Mota, F. L.; Queimada, A. J.; Pinho, S. P.; Macedo, E. A. Aqueous solubility of some natural phenolic compounds. *Ind. Eng. Chem. Res.* **2008**, *47*, 5182–5189.

(66) Nor, M.A.M.; Manan, Z. A.; Mustaffa, A. A.; Suan, C. L. Prediction of the solubility of caffeic acid in water using an activity coefficient model. 1st International Conference on Innovation in Science and Technology. **2015**, 90–95.

(67) Guin, P. S.; Das, S.; Mandal, P. C. Electrochemical reduction of quinones in different media: A Review. *Int. J. Electrochem.* **2011**, *2011*, 1–22.

(68) Giacomelli, C.; Ckless, K.; Galato, D.; Miranda, F. S.; Spinelli, A. Electrochemistry of caffeic acid aqueous solutions with pH 2.0 to 8.5. *J. Braz. Chem. Soc.* **2002**, *13*, 332–338.

(69) Namazian, M.; Zare, H. R. Electrochemistry of chlorogenic acid: experimental and theoretical studies. *Electrochim. Acta.* **2005**, *50*, 4350–4355.